

ECLSS Sustaining Metal Materials Compatibility Final Briefing

Electrochemical and Crevice Corrosion Test Results

Randy Lee

October 6, 2014



JACOBS
ESSSA Group

Agenda, Contents and Scope

- Background and Overview of Materials and Solutions Under Study
- Status and Results of Crevice Wedge/Sandwich Storage Samples (ASTM G78)
 - 100% Complete
- Status and Results of Polarization Corrosion Testing (ASTM G102)
 - Open Circuit Test and Data Analysis – 100% Complete
Provides nondestructive information regarding general corrosion, metal recession and protective oxide formation in real time for a single metal in the test solution. Very slow (no voltage applied).
 - Linear/Tafel Polarization Test and Data Analysis – 100% Complete
Provides nondestructive information regarding general corrosion, metal recession and protective oxide formation under accelerated conditions for a single metal in the test solution (small voltage applied, mV).
 - Cyclic Polarization Data and Test Analysis – 100% Complete
Provides destructive information regarding primarily pitting corrosion, pitting metal recession, protective oxide formation/reformation (passivation/repassivation), oxide breakdown and general corrosion under accelerated conditions for a single metal in the test solution (moderate voltage applied, V).
- Status and Results of Galvanic Corrosion Testing (ASTM G102)
 - Galvanic Coupling Testing – 100% Complete
Provides nondestructive information regarding general corrosion, metal recession and protective oxide formation in real time for two metals interacting across the test solution. Very slow (no voltage applied).

Agenda, Contents and Scope (cont.)

- Summary of Key Points, Conclusions and Comments
- Appendix and Supplemental Topics
 - Examples of Anomalies, Outliers and Extreme Test Conditions

Images and analysis of defects and unusual phenomena observed during extreme polarization conditions. A likely mechanism for the anomalous cathodic behavior in Ni alloys is presented and evaluated.
 - Analytical Methods and Estimation Techniques

Special techniques developed for indicating base metal recession, protective oxide thickness growth rates, evolution of the electrical double layer, oxide breakdown, composition and repassivation factors, long term pitting depth and pitting rate estimates , corrosion susceptibilities and corrosion probability factors.

 - I. Refined Method for the Estimation of Recession and Oxidation Rates
 - II. Special Method for Determination of Electron Exchange Equivalents
 - III. Definition of the Pitting Protection Ratio and the Corrosion Recovery Ratio
 - IV. Definition of Susceptibilities for Corrosion, Pitting Initiation and Sustainment
 - V. Model Development for Pitting Rates and Penetration Depths Over Time
 - VI. Mechanism for Cathodic Behavior During Passivation of High Ni Alloys
 - Description of Events Around the Breakdown Region

Reactions and kinetics pertaining to oxide growth, the passive plateau, film dissolution, *p-n* conductivity and the breakdown region are covered. An overview of the passive multi-layer configuration is presented.

Overview of Materials and Solutions Under Study

- One of the functions of ECLSS is to provide potable water for the crew on the ISS by subjecting human waste liquids through an elaborate recovery process.
- The water extraction procedure begins when raw liquids are ‘pretreated’ with a special acidified stabilizer formula, which ultimately leads to the recovery of about 70% of the water along with the production of concentrated brine which must eventually be discarded.
- Current on-orbit pre-treat solution is suspected of causing calcium precipitates which clog processing filters and reduce water recovery efficiency. Precipitates appear to be due to side reactions associated with the sulfuric acid component in the existing pre-treat formula.
- The proposed pretreat stabilizer is expected to raise the overall liquid processing efficiency to 85% while the sulfuric acid component is replaced with phosphoric acid.
- The new proposed (or ‘alternate’) pretreat formula includes chromic acid (CrO_4^{2-}) and phosphoric acid ($\text{H}_2\text{PO}_4^{1-}$). Test solutions for this study were generated at MSFC. It has been reported that the pretreated test solution contains about 1 ppm CrO_4^{2-} and 20 ppm $\text{H}_2\text{PO}_4^{1-}$, while the brine test solution contains about 5 ppm CrO_4^{2-} and 130 ppm $\text{H}_2\text{PO}_4^{1-}$.
- The purpose of the current compatibility study is to evaluate possible corrosive effects associated with the alternate pretreat and brine solutions when they are in continuous contact with the six metals under study here. A seventh metal, Nitinol 60, has also been proposed and will be evaluated in the future as an addendum to this study.

Overview of Materials and Solutions Under Study

Vendor-Supplied Compositions for the Candidate Metals

Inconel 625		Hastelloy C276		Titanium, CP		Titanium 6Al-4V		Titanium 6Al-4V LI		Cronidur 30	
Raw Wt%		Raw Wt%		Raw Wt%		Raw Wt%		Raw Wt%		Raw Wt%	
Ni	60.3%	Ni	58.9%	Ti	99.5%	Ti	88.4%	Ti	88.5%	Fe	81.8%
Cr	22.3%	Cr	16.1%	O	0.34%	Al	6.26%	Al	6.1%	Cr	15.3%
Mo	9.26%	Mo	15.3%	Fe	0.17%	V	3.95%	V	4.0%	Mo	0.97%
Fe	3.72%	Fe	5.59%			Mo	0.01%	N	0.0102%	Si	0.63%
Nb	3.50%	W	3.39%			N	0.01%	Cr	0.010%	N	0.38%
Co	0.14%							Mo	0.0010%		
Mn	0.13%										
Density	8.44 g/cc	Density	8.89 g/cc	Density	4.51 g/cc	Density	4.42 g/cc	Density	4.42 g/cc	Density	7.70 g/cc

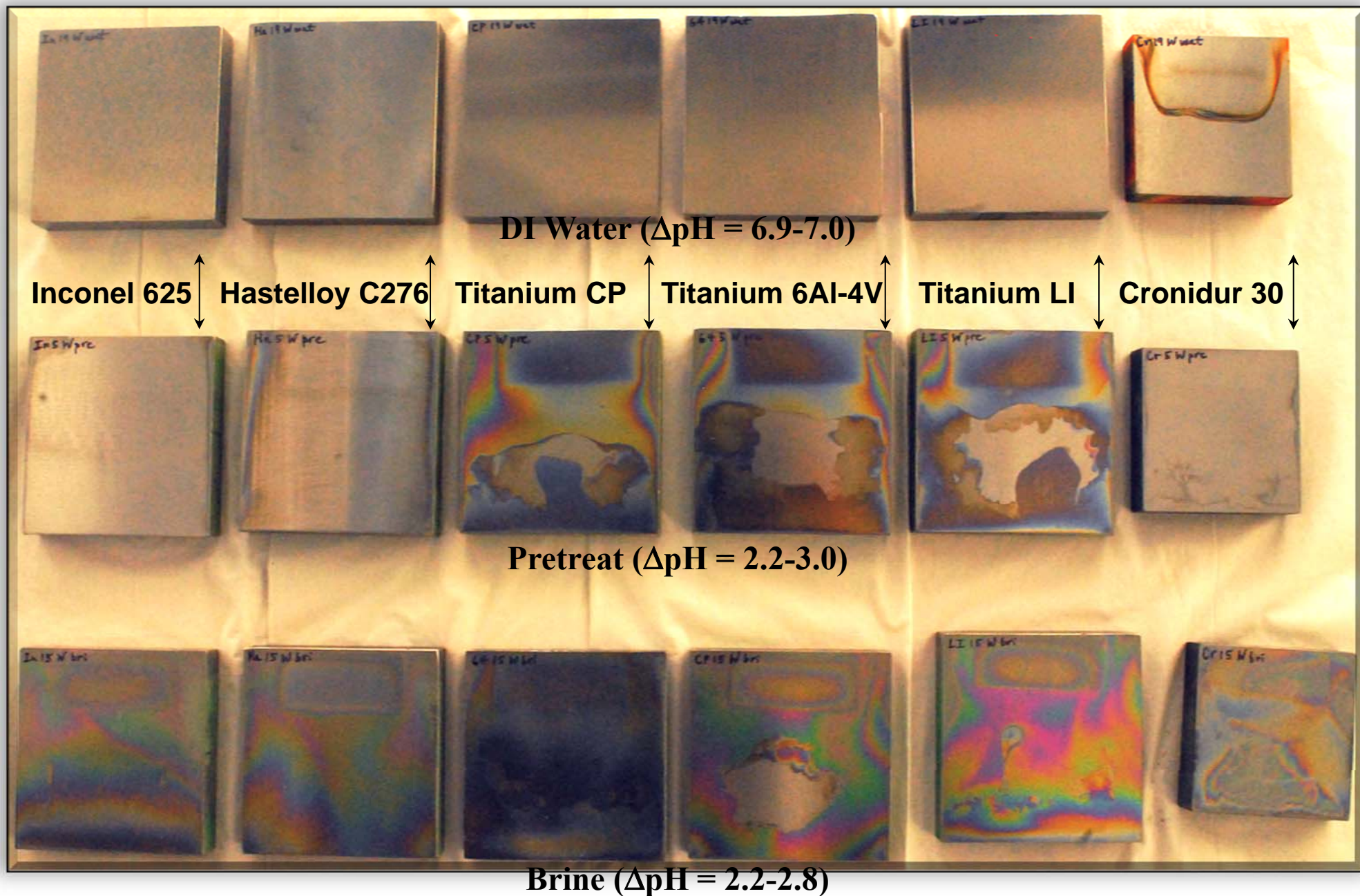
- All six metal candidates are located at the top of most published Galvanic Tables, including the Galvanic Series in Seawater in MIL-STD-889. They are all well documented to be highly resistant to general and pitting corrosion without the requirement for additional surface protection measures because . . .
- All six metals spontaneously form tenacious, self-repairing, passive oxide layers on their surfaces which remarkably protect the base metal from corrosive environments.
- Materials in the Inconel and Hastelloy families are generally recognized as ‘superalloys’. Titanium and most its alloys form the most protective oxide layer of all. Titania deposition technologies are highly sought after for superior corrosion protection on other metals, even without its self-repairing capability.
- Due to the high chromium content, Cronidur could be considered as a ‘super stainless steel’. In passive form, all six metals are similar in nobility to that of silver as clearly reflected in the Galvanic Series.

Status and Results of Wedge and Sandwich Testing

- ❑ **Wedge Sample Configuration**: Sandwich-type assemblies consist of two sample plates clamped together and separated by a small rectangular-shaped layer of filter paper near one side of the clamped assembly to create a tiny *angled crevice gap* between the two plates.
- ❑ **Sandwich Sample Configuration**: Sandwich-type assemblies consist of two sample plates clamped together and separated by a larger square-shaped layer of filter paper centered in the assembly to create a tiny *parallel crevice gap* around the edges between the two plates.
- Assemblies of each of the six metals were placed in storage in both the pretreat and brine solutions for 6 months and 12 months. After each period, they were removed and visually inspected. Six month test results were presented in the Mid-Term Briefing and indicated no corrosion issues. Results of the twelve month samples were identical to the six month group.
- In all cases, microscopic examination indicated no visible signs of pitting, etching, recession or surface growth on any of the six metals in either of the two test solutions.
- Some of the samples developed translucent surface discolorations in the oxide layer after rinsing with pH 7 water. All indications are these patterns are purely optical in nature due to small changes in the dried electrical double layer as the oxide adapts to ambient conditions and have nothing to do with the corrosion protection properties of the metals.
- During the first 6 month period, the pH of the pretreat solution changed from about 2.2 to about 3.0 and that of the brine changed from about 2.2 to 2.8. After one year in storage, final pH values of the test solutions were about 3.9 and 3.3 respectively.

Status and Results of Wedge and Sandwich Testing

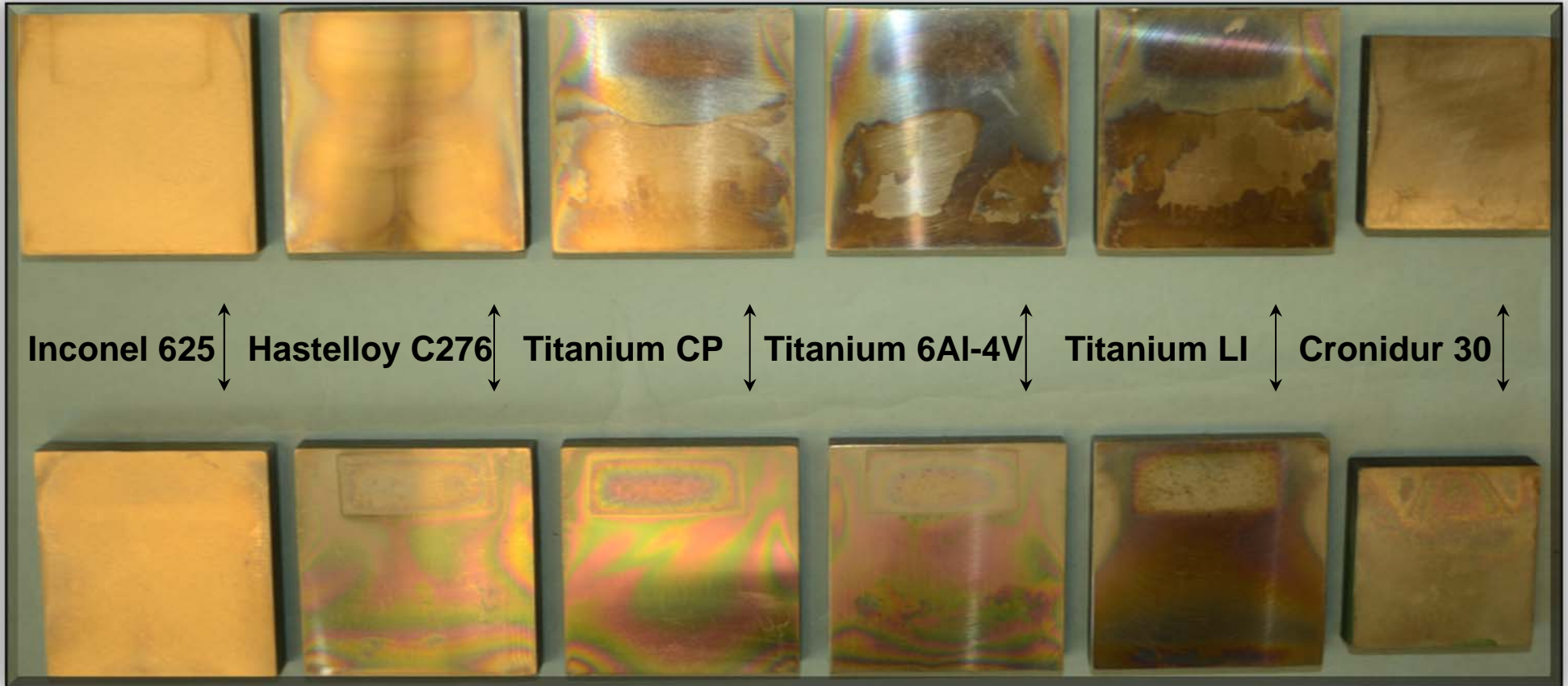
Wedge Samples – 6 Months



Status and Results of Wedge and Sandwich Testing

Wedge Samples – 12 Months

Pretreat ($\Delta\text{pH} = 2.2\text{-}3.9$)

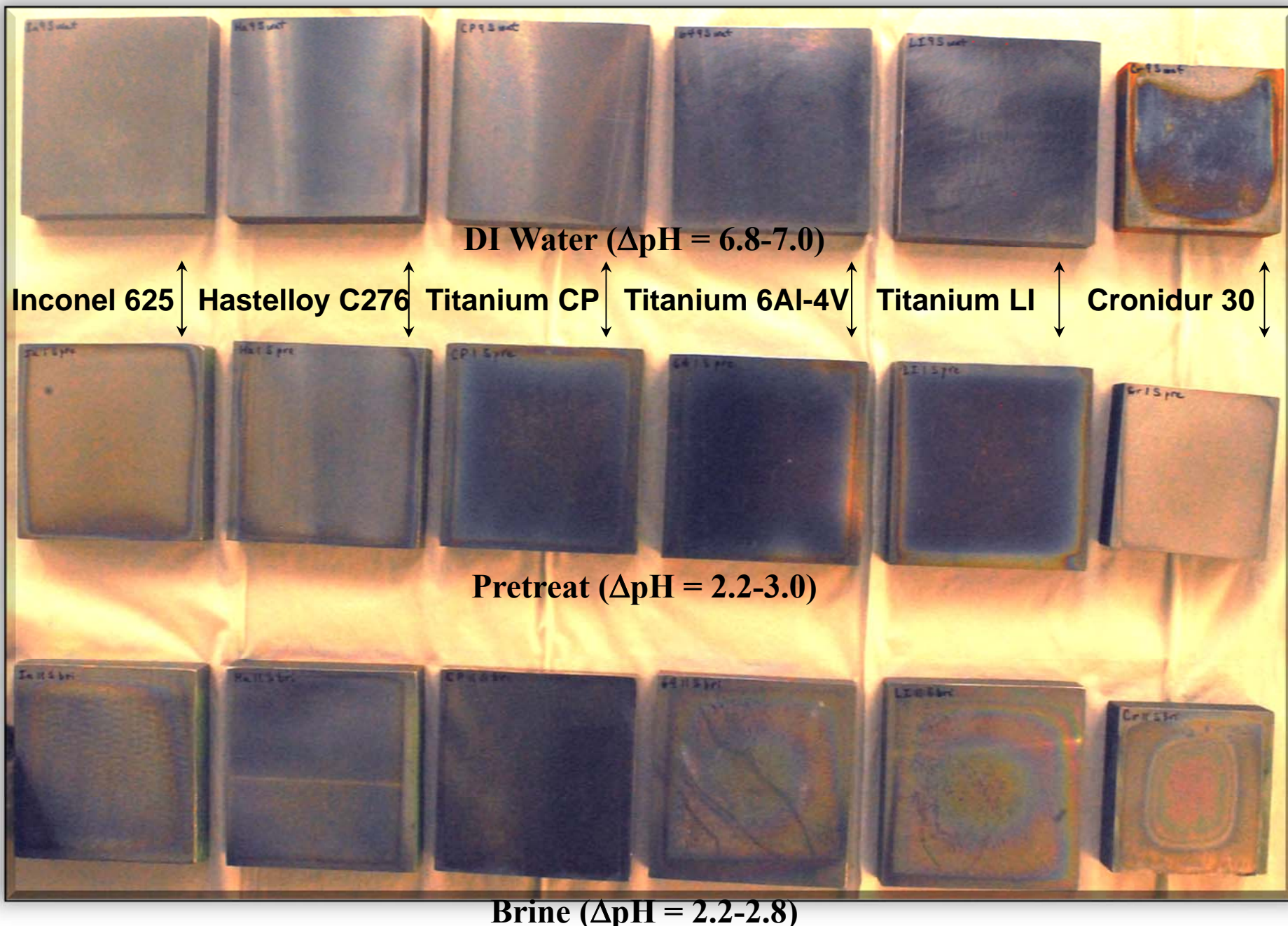


Brine ($\Delta\text{pH} = 2.2\text{-}3.3$)

There is no visible difference between the samples stored for 6 months and those stored for 1 year except the superficial coloration patterns which are considered to be inconsequential.

Status and Results of Wedge and Sandwich Testing

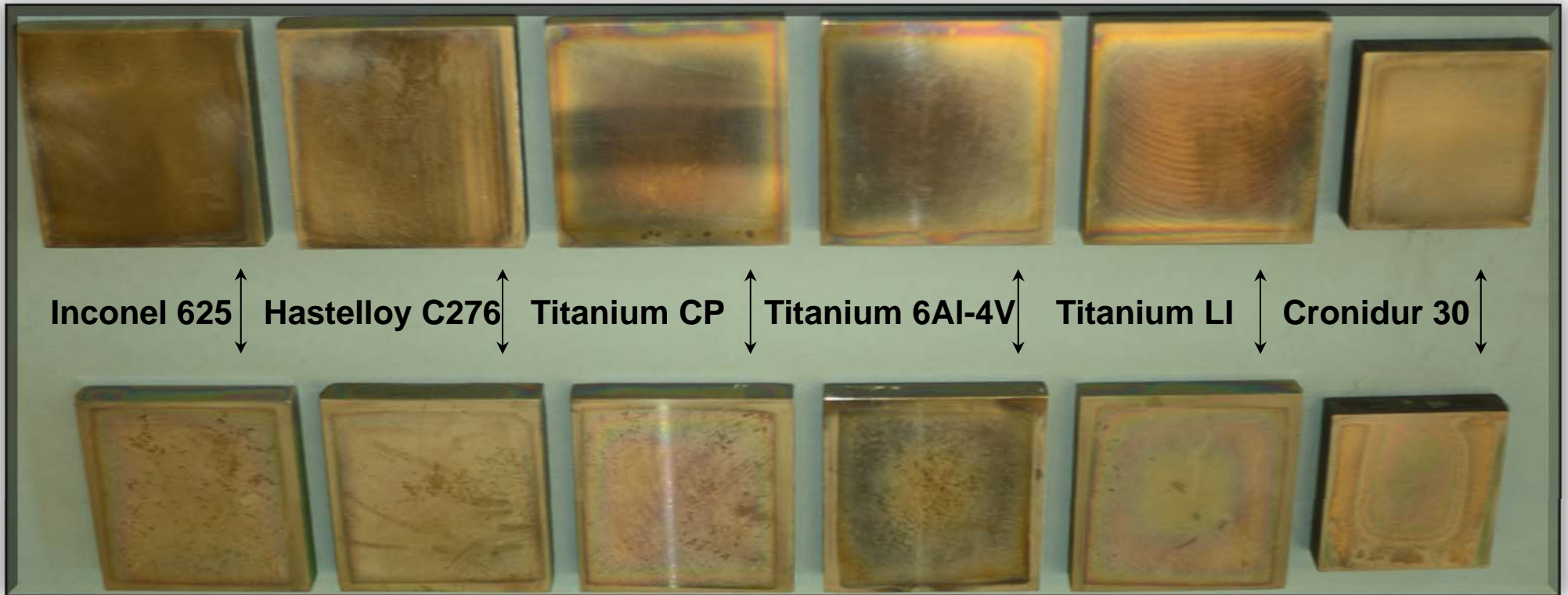
Sandwich Samples – 6 months



Status and Results of Wedge and Sandwich Testing

Sandwich Samples – 12 months

Pretreat ($\Delta\text{pH} = 2.2\text{-}3.9$)

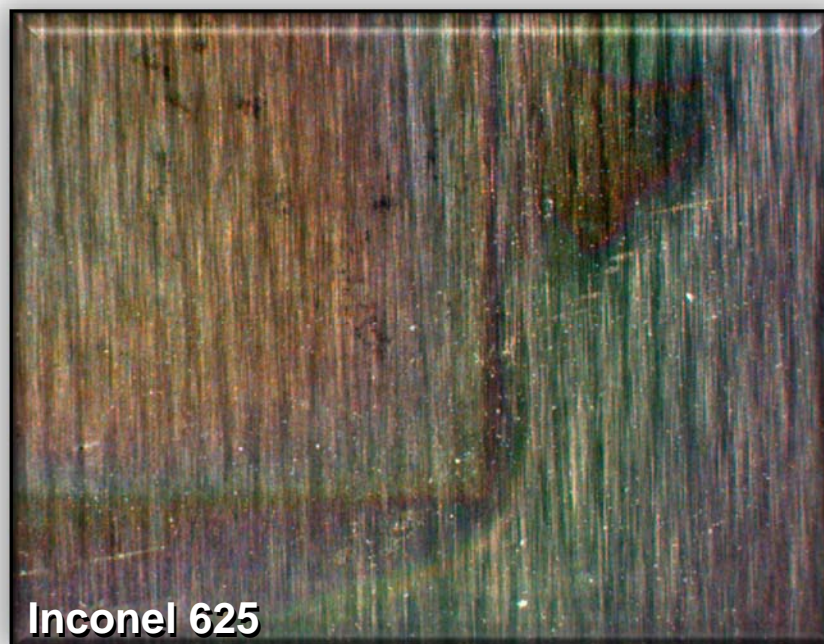
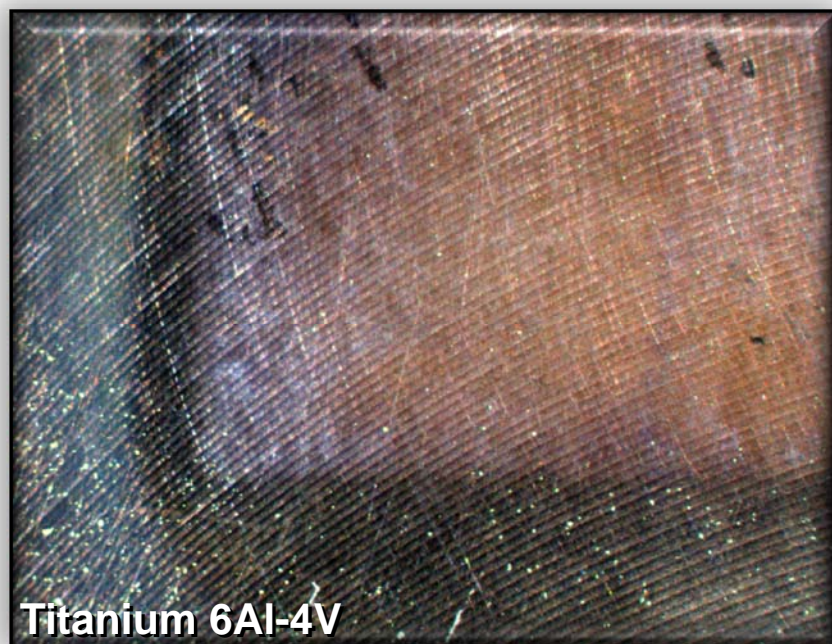
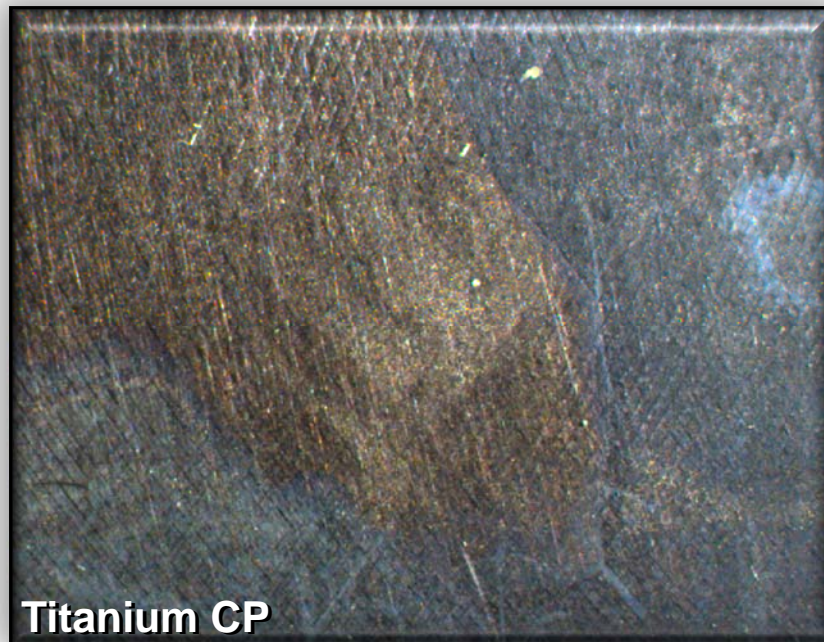
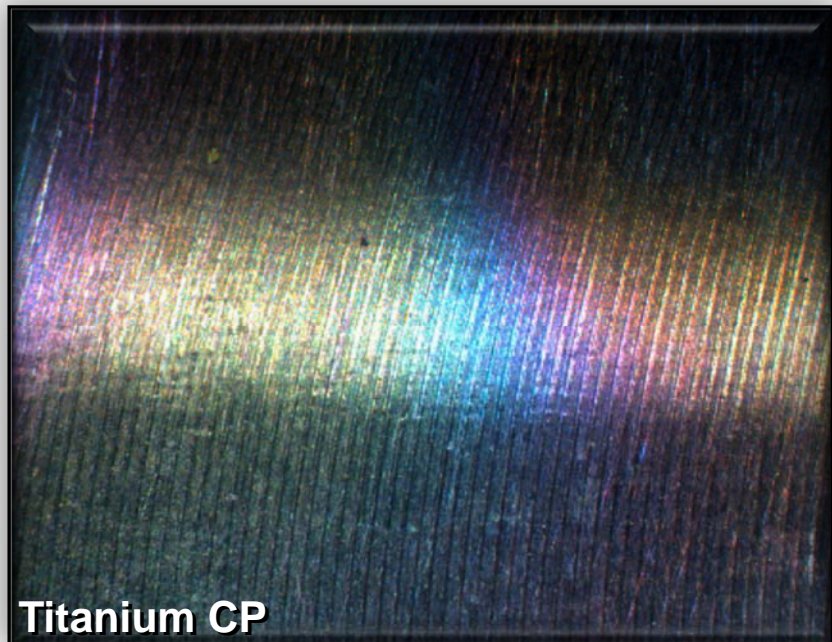


Brine ($\Delta\text{pH} = 2.2\text{-}3.3$)

There is no visible difference between the samples stored for 6 months and those stored for 1 year except the superficial coloration patterns which are considered to be inconsequential.

Status and Results of Wedge and Sandwich Testing

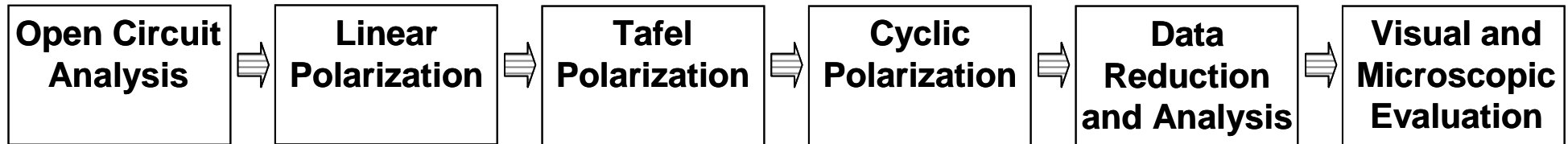
Close-Up of Surface Discolorations



Status and Results of Polarization Testing

Test Sequence Used for Polarization Testing

Each metal candidate was subjected multiple times to . . .



Reported averages are based on 3-6 test runs per metal candidate throughout the study

- Whenever the potential (voltage) and current (amperage) are measured and evaluated together, potential is an indication of the nobility with respect to the tendency, probability or susceptibility for corrosion to occur, while current is directly proportional to the rates of corrosion and oxidation. The latter is typically converted into units that indicate how fast the base metal is recessing/etching and how fast the oxide thickness is growing. Base metal recession and surface oxidation (passivation) are mutually inclusive processes.
- A high breakdown potential for a given metal infers high nobility and low susceptibility to corrosion, while a large pitting current indicates a high pitting rate. A low corrosion potential implies high susceptibility to corrosion while a high repassivation current demonstrates a rapid oxide-restoration process characteristic of metal with a robust protection mechanism.
- For this study, polarization test requirements utilized four highly specialized workstations, each comprised of a complex test unit called a ‘potentiostat’ or ‘galvanostat’ controlled by a computer running specialized polarization testing and data collection software.

Status and Results of Polarization Testing

Equipment Used for Polarization Testing

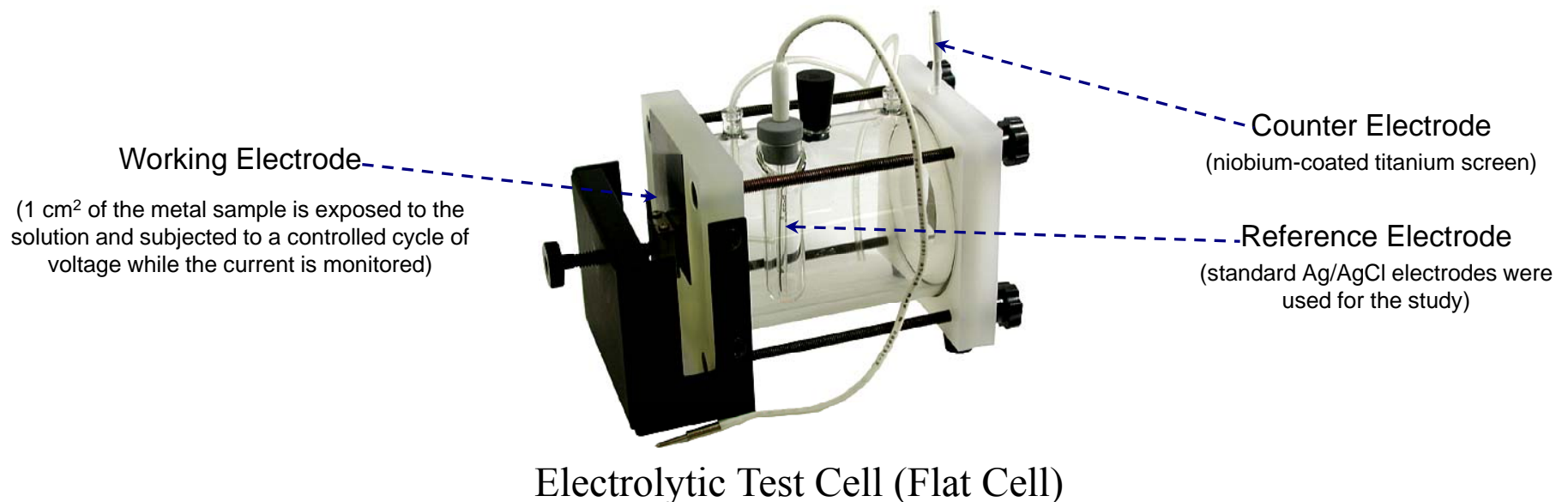
Polarization Test Instrumentation provided by Princeton Applied Research (PAR)



PAR Model 2273 Potentiostat/Galvanostat
(issued in 2004)



PAR Model 273A Potentiostat/Galvanostat
(circa 1985)



Working Electrode

(1 cm² of the metal sample is exposed to the solution and subjected to a controlled cycle of voltage while the current is monitored)

Counter Electrode

(niobium-coated titanium screen)

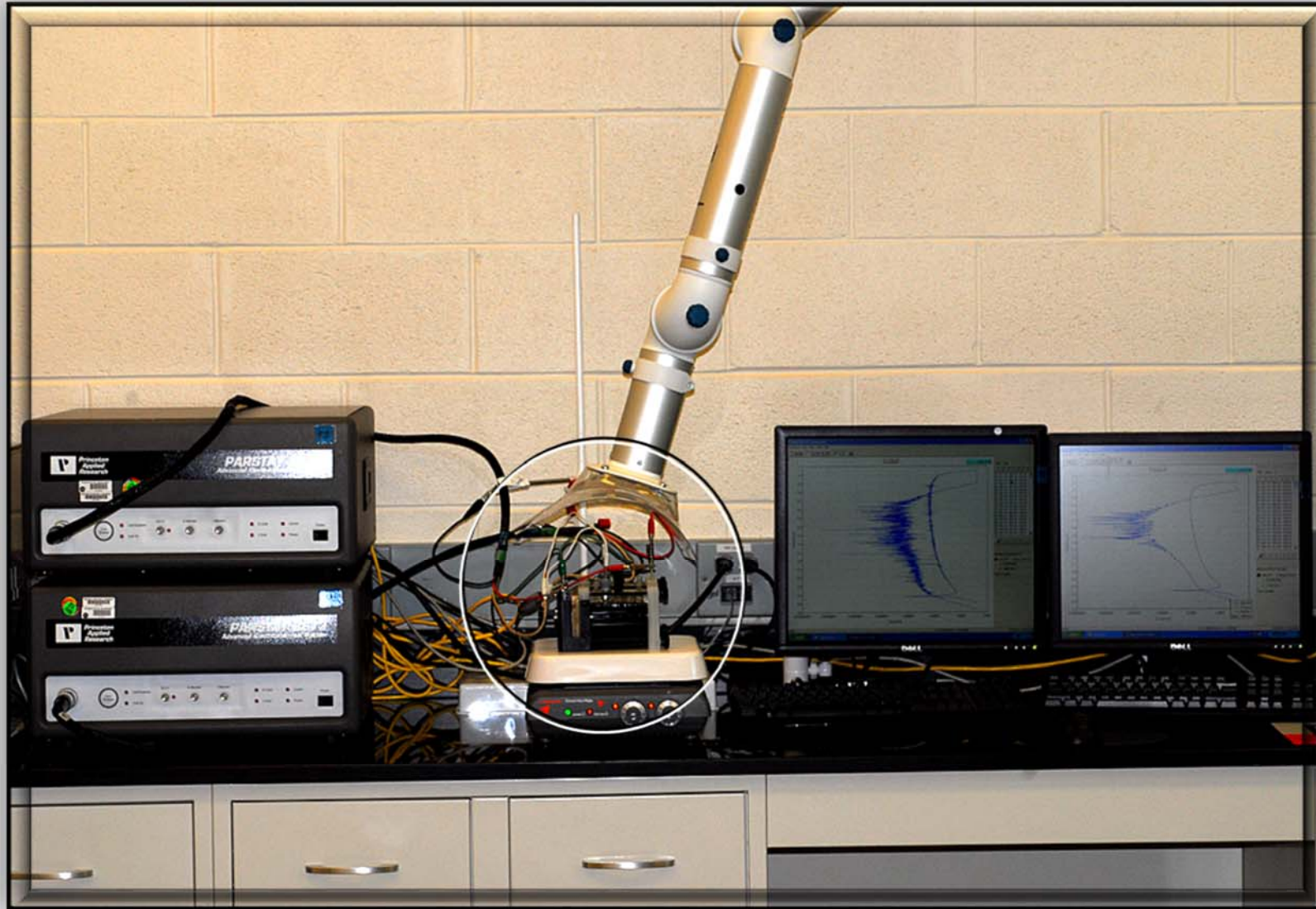
Reference Electrode

(standard Ag/AgCl electrodes were used for the study)

Electrolytic Test Cell (Flat Cell)

Status and Results of Polarization Testing

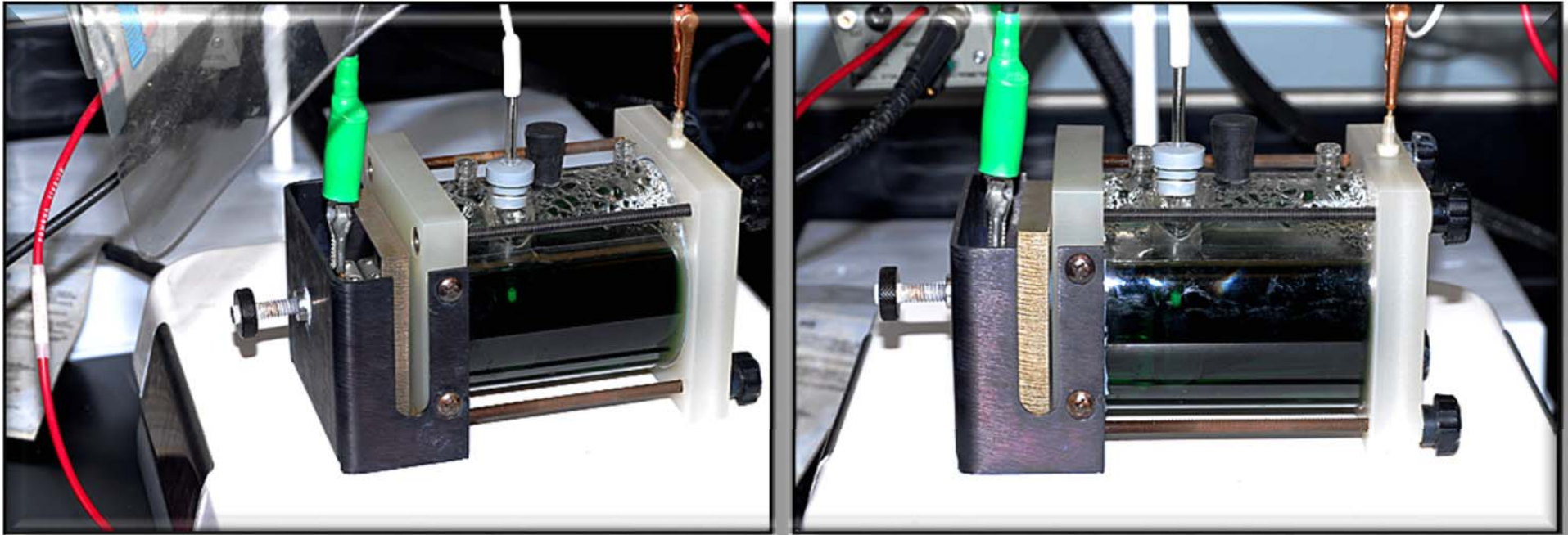
Polarization Workstation Configuration



Two stacked PAR 2273 units are shown on the left side connected to two flat cells on a hotplate in the center. Each 2273 unit is interfaced to a computer (monitors on right). Testing is controlled by the PAR PowerSuite software and test temperature solution is maintained at $100^{\circ}\text{F} \pm 3^{\circ}$.

Status and Results of Polarization Testing

Flat Test Cell Configuration



- Flat test cell containing Pretreat solution with a test sample undergoing cyclic polarization. Ag/AgCl reference electrodes were used throughout. The counter electrode supplies or absorbs electrons as needed while the test sample interacts directly with the test solution.
- The flat cell offers flexibility for a variety of DC electrochemical studies including Open Circuit, Linear, Tafel, Cyclic polarization and Galvanic Coupling measurements.
- For Galvanic Coupling tests, the cell is re-assembled using a second 1cm² sample area end-cap for the other metal so that both samples are connected across the test solution. The second metal is grounded and interacts with the first metal which becomes the anode.

Status and Results of Polarization Testing

Definition and Sequence of Potentiodynamic Testing

- **Open Circuit Analysis** – Measures the steady state potential (voltage) E_{OC} and current I_{OC} as a single metal is exposed to the solution over time with no power applied. Can take more than 10 days to reach stabilization for the noble metals under study.
- **Linear Polarization** – Measures the resulting current response when a very small voltage is applied (± 10 - 20 mV). This level is considered to be nondestructive. Provides the corrosion resistance R_{Cor} and the corrosion rate k_{Cor} in the preselected potential range.
- **Tafel Polarization** – Measures current response across a larger potential range (± 200 - 250 mV). Spans the early cathodic and anodic regions providing the corrosion potential E_{Cor} , corrosion current I_{Cor} , the Tafel parameters and k_{Cor} . Essentially nondestructive.
- **Cyclic Polarization** – Applies a broad preselected potential cycle across the anodic passivation range and beyond the breakdown point E_{Brk} . The run is then reversed and brought back down through the repassivation branch, all while the current is monitored. A hysteresis loop is often generated. Provides rates and information regarding passivation, pitting, repassivation, oxide protection and general corrosion properties.
- **Galvanic Coupling** – Measures the steady state potential (voltage) E_{OC} and current I_{OC} as two metals interact (galvanically) across the test solution with no power applied. Can take more than 10 days to reach stabilization for the noble metals under study.

Status and Results of Electrochemical Testing

- **Status:** All Open Circuit, Linear, Tafel and Cyclic Polarization tests have been completed for both solutions and the results were presented in the Mid-Term Briefing. All Galvanic Coupling tests have now been completed and are presented in this Final Briefing.

Results Overview

- **General Corrosion:** All six metals exhibited *insignificant* corrosion rates and very pronounced surface oxide passivation/repassivation protection mechanisms in both test solutions. Recession rates for these metals are due to growth of the protective oxide layer rather than corrosive degradation of the base metal. They are all very corrosion-resistant.

All six metals appear to be at least one order of magnitude higher than the ‘Outstanding’ rating for general corrosion which is the most noble rating recognized in the industry. The Inconel, Hastelloy and Cronidur samples exhibited nobilities very close that of Titanium in accordance with published Galvanic Series in seawater. All metals were comparable to silver.
- **Pitting Corrosion:** None of the metals exhibited any signs of pitting under non-accelerated conditions of exposure where minimal or no voltage was applied. However . . .

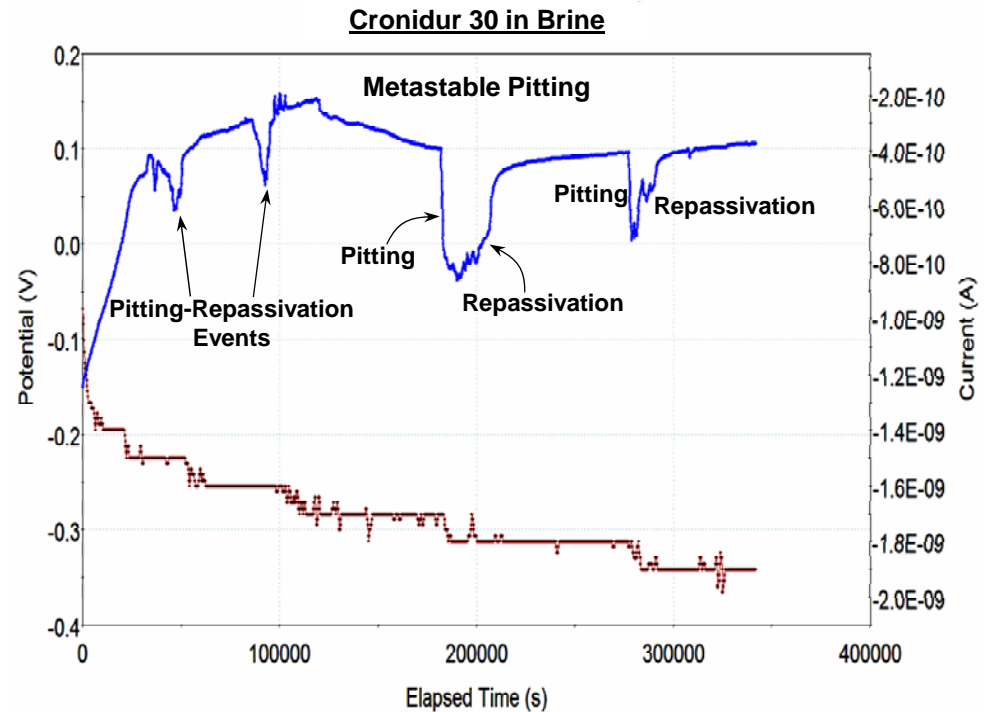
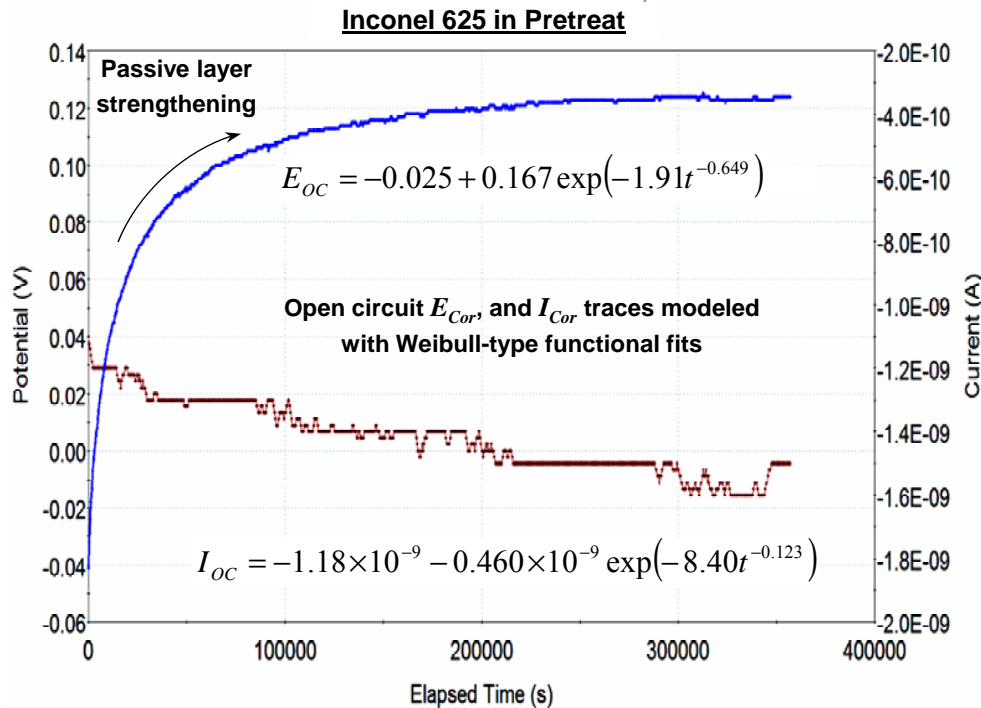
Under more aggressive cyclic polarization conditions, minor pitting was indicated on some of the Cronidur Pretreat samples, while pitting occurred on *all* the Cronidur Brine samples under extreme test conditions. Cyclic polarization data analysis reflects these observations.
- **Galvanic Coupling:** While data averages indicate ranking differences between the couples, none of the metals exhibited any signs of visible surface degradation. Corrosive effects due to coupling are considered to be completely insignificant as these tests appear to demonstrate what is already well established... that all six metals are comparable in nobility.

Status and Results of Polarization Testing

Open Circuit Analysis for General Corrosion

- Open Circuit Analysis measures the steady state potential E_{OC} and current I_{OC} as the sample is exposed to the solution over time with no power applied. OC measurements reveal real-time general corrosion properties but may sometimes indicate pitting tendencies as well.
- Transients may reflect reactions associated with general corrosion, pitting events and passivation/repassivation, as well as compositional, electrical and micro-structural modifications associated with the electrical double layer, the outer oxide-hydroxide layer and the inner metal oxide layer as these structures evolve and adapt to the solution over time.

Examples of Actual Test Runs and Analysis



Status and Results of Polarization Testing

Open Circuit Summary and Analysis for General Corrosion

Apparent Relative Nobility

Oxidation Rates at Steady State

Stabilization Period

Relative Corrosion Susceptibility

Rates for General Corrosion-Recession & Oxidation (Not Pitting)

Time To Reach Equilibrium
(How fast the oxide adapts to the solution)

Ranked from highest nobility	PreTreat		Ranked from lowest recession rate	PreTreat				Ranked from low stabilization time	~ 90% of Steady State (hours)
	Steady State Potential (mV _{AgCl})	Susceptibility to General Corrosion		Metal Recession Analogous to "Corrosion Rate" (Å/day)	Oxide Growth/Dissolution Includes recession plus outward growth (mil/year)	Oxide Growth/Dissolution (Å/day)	Oxide Growth/Dissolution (mil/year)		
Titanium CP	125.0	0.03%	Titanium 6-4 LI	9.26	0.0133	24.1	0.0347	Titanium CP	5
Titanium 6-4 LI	121.6	0.08%	Titanium CP	9.64	0.0139	27.8	0.0399	Titanium 6-4 LI	6
Titanium 6Al-4V	102.9	0.09%	Titanium 6Al-4V	9.90	0.0143	28.8	0.0413	Titanium 6Al-4V	7
Cronidur 30	93.4	0.75%	Cronidur 30	17.2	0.0248	87.2	0.1253	Hastelloy C-276	13
Hastelloy C-276	92.7	0.72%	Hastelloy C-276	27.4	0.0393	139	0.2004	Inconel 625	15
Inconel 625	85.5	0.70%	Inconel 625	30.1	0.0432	158	0.2277	Cronidur 30	19

Open Circuit Potential

Commonly reported as "Corrosion Rate"

At Steady State, oxide growth rate and dissolution rate are equal

Ranked from highest nobility	Brine		Ranked from lowest recession rate	Brine				Ranked from low stabilization time	~ 90% of Steady State (hours)
	Steady State Potential (mV _{AgCl})	Susceptibility to General Corrosion		Metal Recession Analogous to "Corrosion Rate" (Å/day)	Oxide Growth/Dissolution Includes recession plus outward growth (mil/year)	Oxide Growth/Dissolution (Å/day)	Oxide Growth/Dissolution (mil/year)		
Titanium CP	145.2	0.03%	Titanium CP	3.07	0.00442	7.22	0.0104	Titanium CP	9
Titanium 6-4 LI	132.1	0.08%	Titanium 6Al-4V	3.52	0.00505	9.01	0.0129	Titanium 6Al-4V	11
Titanium 6Al-4V	126.8	0.08%	Titanium 6-4 LI	3.75	0.00539	9.59	0.0138	Titanium 6-4 LI	12
Hastelloy C-276	114.3	0.76%	Cronidur 30	6.03	0.00866	32.1	0.0461	Hastelloy C-276	21
Inconel 625	102.5	0.66%	Hastelloy C-276	11.5	0.01656	41.3	0.0594	Inconel 625	25
Cronidur 30	89.7	0.65%	Inconel 625	12.3	0.01766	44.2	0.0636	Cronidur 30	33

Open Circuit Potential

Commonly reported as "Corrosion Rate"

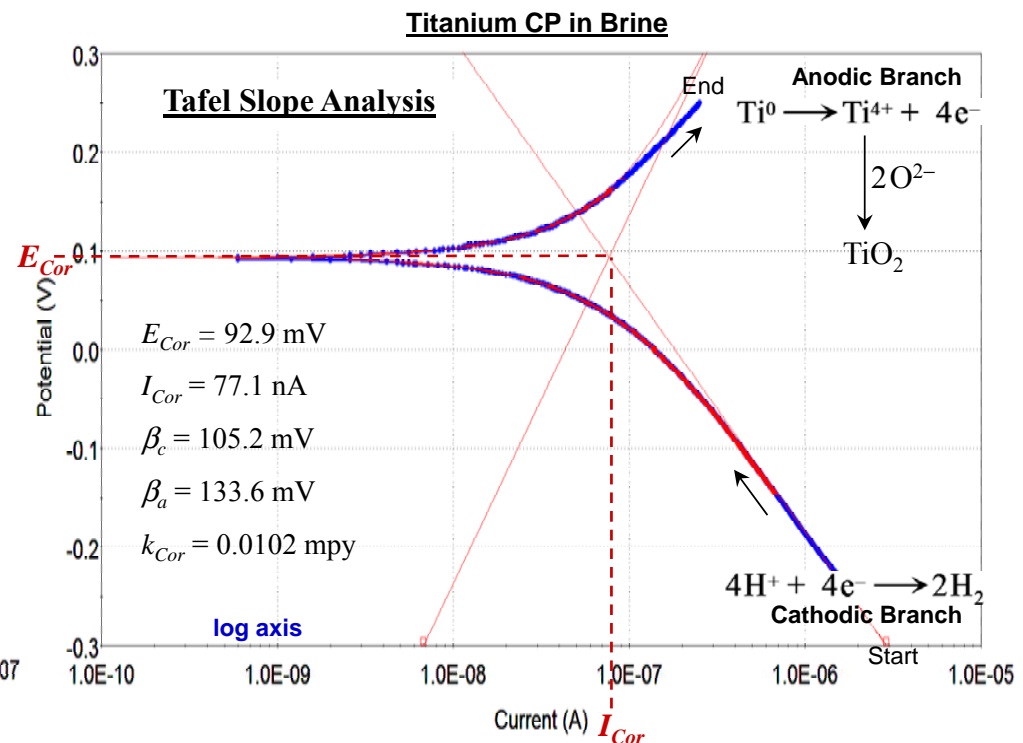
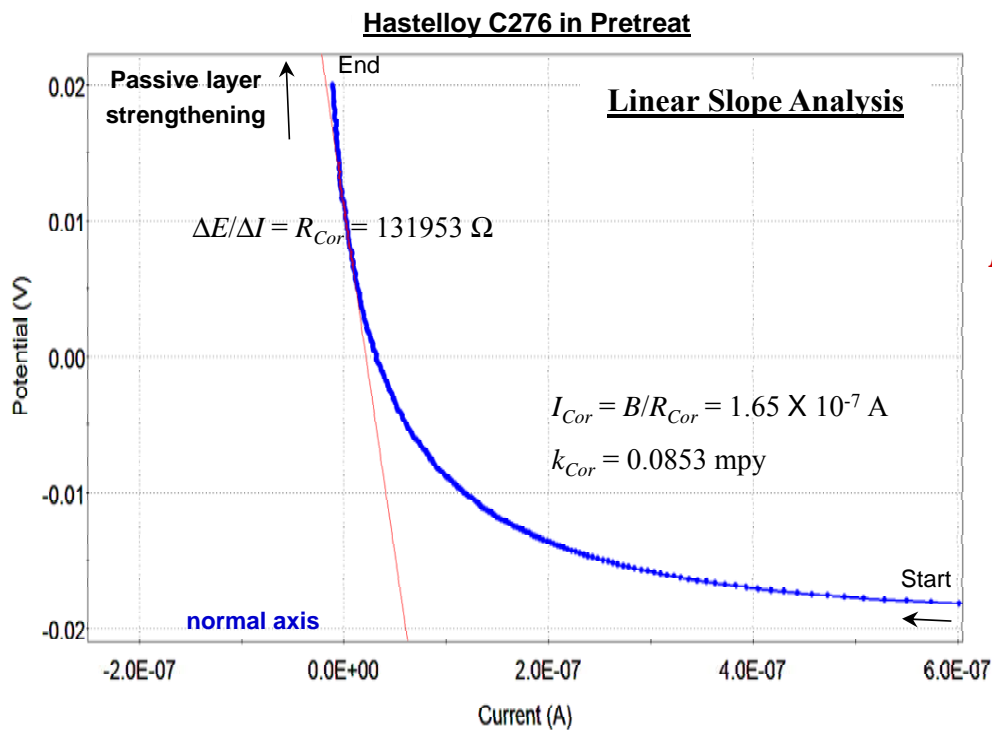
At Steady State, oxide growth rate and dissolution rate are equal

Status and Results of Polarization Testing

Linear and Tafel Analysis for General Corrosion

- Linear Polarization measures the resulting current response when a small voltage is applied ($\pm 10\text{-}20$ mV). Provides the corrosion resistance R_{Cor} , corrosion current I_{Cor} and the corrosion rate k_{Cor} in the preselected potential range. These values permit the estimation of rates for general recession depth into the base metal and oxide thickness growth.
- Tafel Polarization measures the current across a wider potential range ($\pm 200\text{-}250$ mV). Spans the early cathodic and anodic regions providing values for E_{Cor} , I_{Cor} , k_{Cor} and the primary Tafel parameters β_a and β_c which supplement the Linear measurements.

Examples of Actual Test Runs and Analysis



Status and Results of Polarization Testing

Combined Linear and Tafel Polarization Summary for General Corrosion

Apparent Relative Nobility

Under Slight Polarization

Accelerated Oxidation Rates at E_{Corr}

Rates for General Corrosion-Recession & Oxidation under Slight Polarization (General Corrosion, Not Pitting)

PreTreat			PreTreat			PreTreat			
Ranked from highest nobility	Corrosion Potential (mV _{AgCl})	Susceptibility to General Corrosion	Ranked from lowest recession rate	Corrosion Resistance (MΩ/cm ²)	Corrosion Current (nA/cm ²)	Metal Recession Commonly reported as "Corrosion Rate"		Anodic Oxide Growth Includes recession plus outward growth	
						(Å/day)	(mil/year)	(Å/day)	(mil/year)
Titanium CP	102.0	0.10%	Titanium 6-4 LI	1.13	42.3	9.34	0.0134	27.0	0.0387
Titanium 6-4 LI	97.5	0.34%	Titanium CP	1.03	41.2	9.55	0.0137	27.5	0.0395
Titanium 6Al-4V	96.2	0.35%	Titanium 6Al-4V	0.86	39.0	9.74	0.0140	25.4	0.0365
Inconel 625	78.8	3.25%	Cronidur 30	0.09	298	37.8	0.0534	192	0.2750
Hastelloy C-276	77.3	3.42%	Hastelloy C-276	0.07	484	63.4	0.0911	323	0.4643
Cronidur 30	76.3	3.26%	Inconel 625	0.06	583	75.5	0.1084	397	0.5712

E_{Corr}

R_{Corr}

I_{Corr}

Commonly reported as "Corrosion Rate"

Includes recession plus outward growth

Brine			Brine			Brine			
Ranked from highest nobility	Corrosion Potential (mV _{AgCl})	Susceptibility to General Corrosion	Ranked from lowest recession rate	Corrosion Resistance (MΩ/cm ²)	Corrosion Current (nA/cm ²)	Metal Recession Commonly reported as "Corrosion Rate"		Anodic Oxide Growth Includes recession plus outward growth	
						(Å/day)	(mil/year)	(Å/day)	(mil/year)
Titanium 6-4 LI	128.7	0.24%	Titanium CP	3.33	26.4	6.35	0.0091	18.3	0.0263
Titanium CP	120.2	0.08%	Titanium 6-4 LI	2.89	28.0	6.57	0.0095	19.0	0.0273
Titanium 6Al-4V	111.9	0.29%	Titanium 6Al-4V	1.18	29.0	6.60	0.0095	17.2	0.0247
Hastelloy C-276	84.1	3.05%	Cronidur 30	0.25	202	23.1	0.0331	117	0.1677
Cronidur 30	83.0	2.94%	Hastelloy C-276	0.20	333	43.6	0.0627	222	0.3194
Inconel 625	81.5	3.11%	Inconel 625	0.17	430	55.6	0.0799	293	0.4210

E_{Corr}

R_{Corr}

I_{Corr}

Commonly reported as "Corrosion Rate"

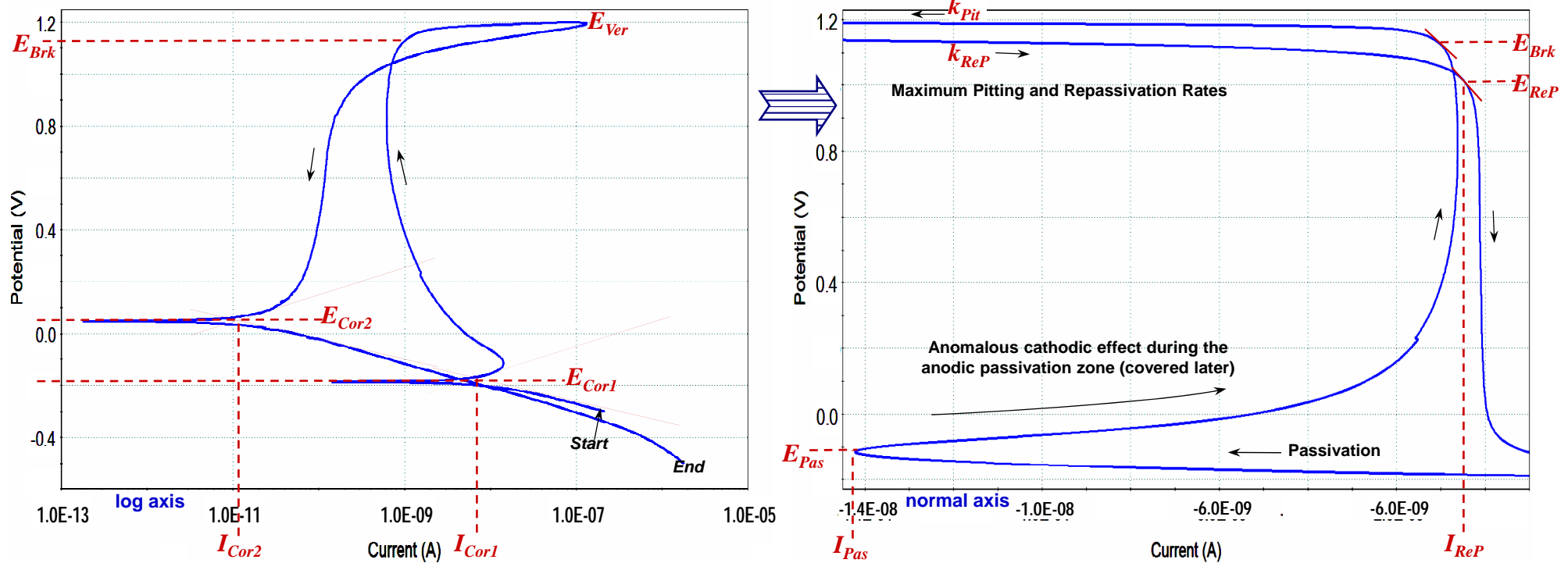
Includes recession plus outward growth

Status and Results of Polarization Testing

Cyclic Polarization Analysis for General and Pitting Corrosion

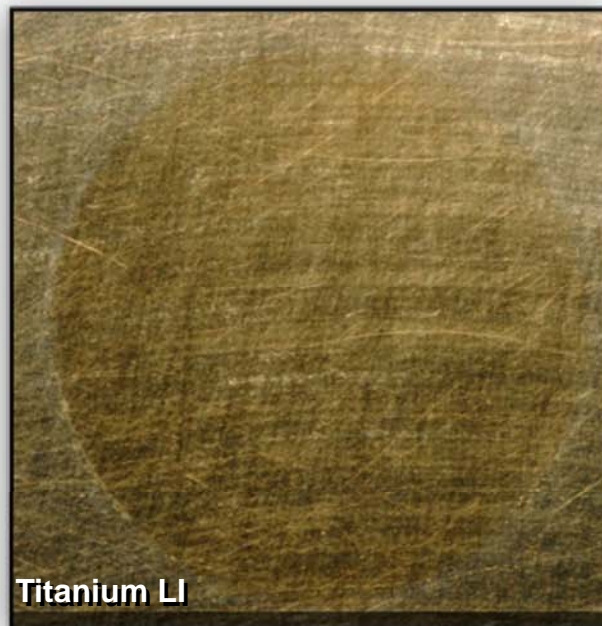
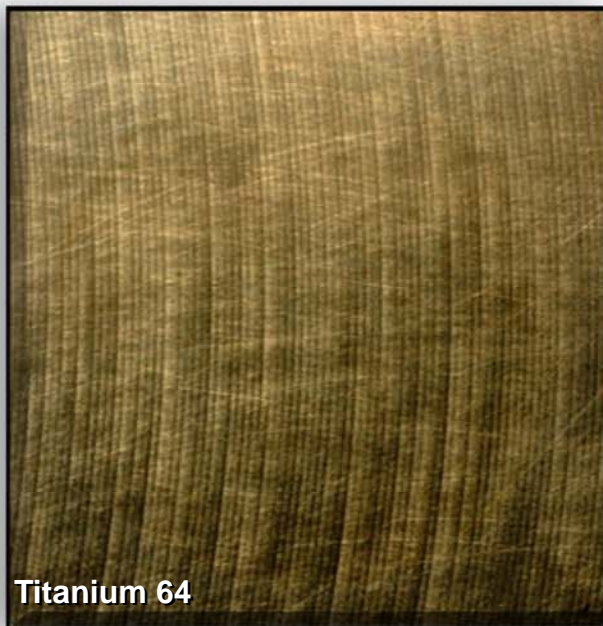
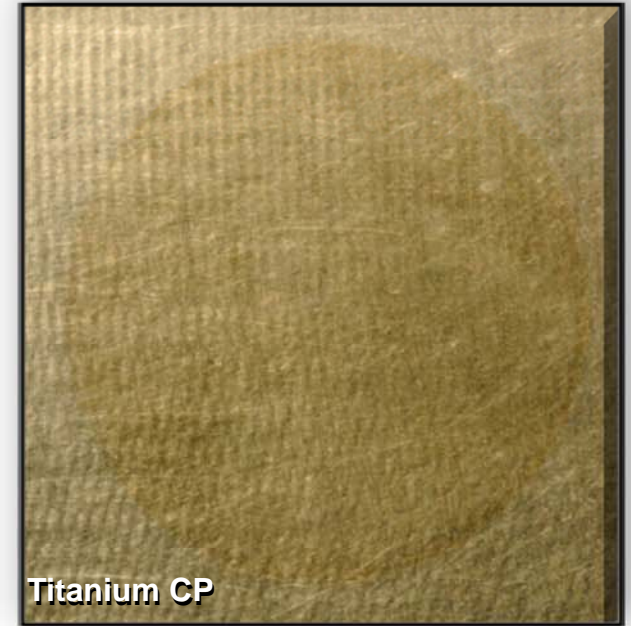
- This test is configured to begin at a point slightly cathodic to E_{OC}/E_{Cor} and applies an increasing voltage along a pre-selected ramp through the passivation potential E_{Pas} , beyond the breakdown point E_{Brk} to a preselected vertex E_{Ver} , where the potential ramp reverses and begins to decrease hysteretically, passing through the repassivation potential E_{ReP} , and the recovery region at E_{Cor2} . Provides pitting, crevicing and general corrosion information.
- An advanced approach was pursued which utilized both the log and normal data curves to obtain E_{Cor1} , E_{Cor2} , I_{Cor1} , I_{Cor2} , E_{Pas} , E_{Brk} , E_{ReP} , k_{Pas} , k_{Pit} , k_{ReP} and several other key factors.

Example: Hastelloy C276 in Brine



Status and Results of Polarization Testing

Pretreat: Typical Sample Areas After Polarization Testing and DI Water Rinse



Status and Results of Polarization Testing

Brine: Typical Sample Areas After Polarization Testing and DI Water Rinse



Status and Results of Polarization Testing

Cyclic Polarization Summary and Analysis for Pitting Corrosion

Potentials & Rates Associated With
Pitting Corrosion & Pitting Protection

Indications & Probabilities Associated With
Pitting Corrosion & Pitting Protection

Ranked from lowest Pitting Susceptibility to highest

Ranked from lowest Pitting Susceptibility	<u>PreTreat</u>		<u>PreTreat</u>			Area of Hysteresis Loop (mV-mA)	Pitting Recovery Ratio (k_{Pit} / k_{Rep})	Corrosion Recovery Ratio (k_{Cor1} / k_{Cor2})	<u>PreTreat</u>	
	Maximum Passivation Potential (mV _{AgCl})	Oxide Breakdown Potential (mV _{AgCl})	Maximum Repassivation Potential (mV _{AgCl})	Maximum Gross Pitting Rate (mil/year)	Maximum Repassivation Rate (mil/year)				Susceptibility for Pitting Initiation $f(E_{Brk} - E_{Pas})$	Susceptibility for Pitting Sustainment $f(E_{Brk} - E_{Rep})$
Titanium CP	506	1833	1717	0.73	4.28	-479	0.20	123	1.25%	0.06%
Titanium 6Al-4V	560	2000	1704	0.76	3.33	-406	0.19	10.5	1.53%	0.16%
Titanium 6-4 LI	864	2314	1904	0.77	4.04	-463	0.20	6.5	1.76%	0.20%
Inconel 625	-52.5	978	909	1.19	0.57	-3.30	2.01	612	7.33%	1.11%
Hastelloy C-276	-74.7	950	809	1.07	0.52	-3.48	2.04	767	7.79%	1.29%
Cronidur 30	143	956	-5.23	35.3	14.4	+63171	2.23	1.33	14.3%	13.4%

E_{Pas} E_{Brk} E_{Rep} k_{Pit} k_{Rep} Hi neg values = hi resistance to pitting If > 1, sustained pitting possible Hi values offer hi general protection Low sustainment implies good protection with only metastable pitting possible

Ranked from lowest Pitting Susceptibility to highest

Ranked from lowest Pitting Susceptibility	<u>Brine</u>		<u>Brine</u>			Area of Hysteresis Loop (mV-mA)	Pitting Recovery Ratio (k_{Pit} / k_{Rep})	Corrosion Recovery Ratio (k_{Cor1} / k_{Cor2})	<u>Brine</u>	
	Maximum Passivation Potential (mV _{AgCl})	Oxide Breakdown Potential (mV _{AgCl})	Maximum Repassivation Potential (mV _{AgCl})	Maximum Gross Pitting Rate (mil/year)	Maximum Repassivation Rate (mil/year)				Susceptibility for Pitting Initiation $f(E_{Brk} - E_{Pas})$	Susceptibility for Pitting Sustainment $f(E_{Brk} - E_{Rep})$
Titanium CP	960	2109	1729	3.26	17.4	-541	0.19	84.6	1.65%	0.16%
Titanium 6Al-4V	865	2302	1600	3.33	17.5	-486	0.19	3.65	1.76%	0.34%
Titanium 6-4 LI	830	2180	1730	3.52	18.9	-308	0.20	3.55	1.78%	0.23%
Inconel 625	130	1046	858	6.71	3.24	-5.98	2.07	352	8.76%	1.43%
Hastelloy C-276	73.4	903	836	8.53	4.20	-5.06	2.03	476	9.08%	1.64%
Cronidur 30	134	742	186	137	57.5	+71600	2.47	2.59	16.8%	16.6%

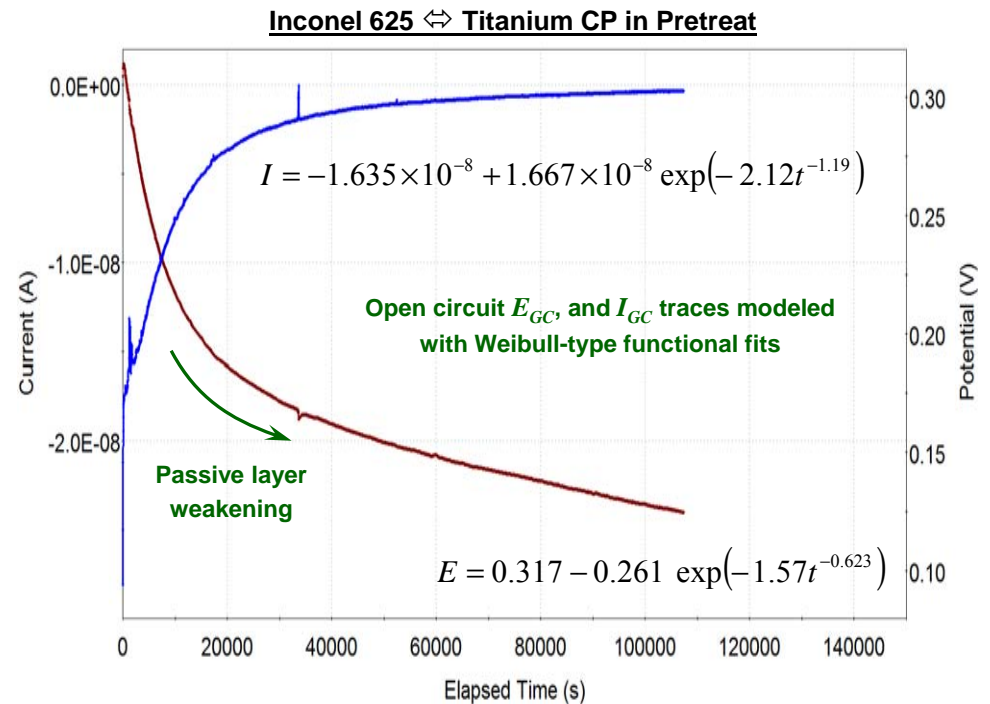
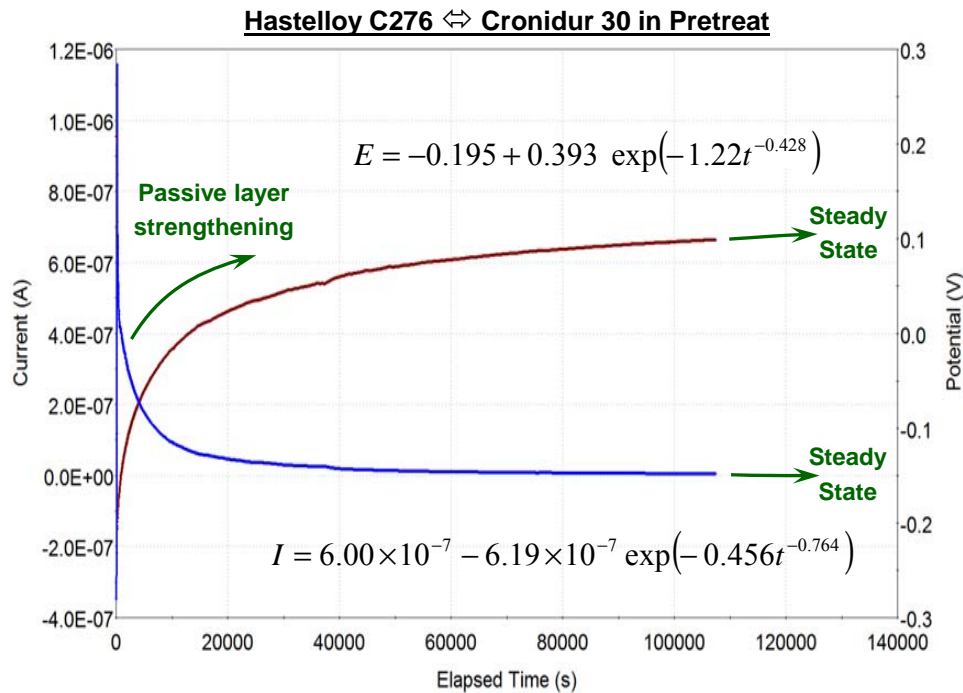
E_{Pas} E_{Brk} E_{Rep} k_{Pit} k_{Rep} Hi neg values = hi resistance to pitting If > 1, sustained pitting possible Hi values offer hi general protection Low sustainment implies good protection with only metastable pitting possible

Status and Results of Galvanic Testing

Galvanic Coupling Analysis for General Corrosion

- Galvanic coupling measurements monitor the steady state potential E_{GC} and current I_{GC} of one metal, the primary test metal, as it is rendered anodic toward a second test metal which is grounded as the two interact across the test solution. Data is collected on the primary metal.
- Transients may reflect reactions associated with general corrosion, pitting events and passivation/repassivation, as well as compositional, electrical and micro-structural modifications associated with the electrical double layer, the outer oxide-hydroxide layer and the inner metal oxide layer as these structures evolve and adapt to the solution over time.

Examples of Actual Test Runs and Analysis



Status and Results of Galvanic Testing

Galvanic Coupling Analysis for Alternate Pretreat Solution

Apparent Relative Nobility and Relative Corrosion Susceptibility			Oxidation Rates at Steady State Apparent Rates for Corrosion-Recession & Oxidation Activity				Stabilization Period Time To Reach ~90% Equilibrium		
PreTreat	Steady State Potential (mV _{AgCl})	Relative Susceptibility to Corrosion	PreTreat	Metal Recession		Anodic Oxide Growth		PreTreat	Induction Period (hours)
				(Å/day)	(mil/year)	(Å/day)	(mil/year)		
Inconel 625 Couples									
Hastelloy C276	127	0.60%	Hastelloy C276	3.24	0.0047	17.1	0.0245	Hastelloy C276	12.5
Titanium CP	78	0.73%	Titanium CP	7.46	0.0107	39.3	0.0565	Titanium CP	3.8
Titanium 6-4	81	0.71%	Titanium 6-4	9.50	0.0137	50.1	0.0720	Titanium 6-4	4.1
Titanium LI	75	0.73%	Titanium LI	8.70	0.0125	45.8	0.0659	Titanium LI	4.4
Cronidur 30	109	0.67%	Cronidur 30	2.59	0.0037	13.6	0.0196	Cronidur 30	8.0
Hastelloy C276 Couples									
Inconel 625	147	0.60%	Inconel 625	2.82	0.0040	13.9	0.0199	Inconel 625	12.0
Titanium CP	61	0.83%	Titanium CP	6.01	0.0086	29.6	0.0425	Titanium CP	4.3
Titanium 6-4	77	0.77%	Titanium 6-4	7.27	0.0104	35.8	0.0514	Titanium 6-4	4.5
Titanium LI	70	0.79%	Titanium LI	9.55	0.0137	47.0	0.0676	Titanium LI	4.9
Cronidur 30	147	0.61%	Cronidur 30	3.21	0.0046	15.8	0.0227	Cronidur 30	6.9
Titanium CP Couples									
Inconel 625	127	0.03%	Inconel 625	41.4	0.0594	108	0.1548	Inconel 625	7.4
Hastelloy C276	109	0.03%	Hastelloy C276	31.5	0.0452	81.9	0.1177	Hastelloy C276	8.0
Titanium 6-4	50	0.04%	Titanium 6-4	3.08	0.0044	8.01	0.0115	Titanium 6-4	14.8
Titanium LI	53	0.04%	Titanium LI	3.43	0.0049	8.93	0.0128	Titanium LI	15.1
Cronidur 30	111	0.04%	Cronidur 30	33.1	0.0475	86.1	0.1237	Cronidur 30	9.7
Titanium 6-4 Couples									
Inconel 625	125	0.09%	Inconel 625	45.1	0.0648	130	0.1870	Inconel 625	7.7
Hastelloy C276	122	0.09%	Hastelloy C276	33.8	0.0486	97.6	0.1402	Hastelloy C276	8.3
Titanium CP	55	0.11%	Titanium CP	2.56	0.0037	7.39	0.0106	Titanium CP	14.6
Titanium LI	57	0.11%	Titanium LI	3.30	0.0047	9.51	0.0137	Titanium LI	14.8
Cronidur 30	103	0.09%	Cronidur 30	31.6	0.0454	91.2	0.1311	Cronidur 30	10.2
Titanium LI Couples									
Inconel 625	124	0.08%	Inconel 625	44.3	0.0637	128	0.1835	Inconel 625	8.3
Hastelloy C276	114	0.09%	Hastelloy C276	41.8	0.0600	120	0.1729	Hastelloy C276	9.7
Titanium CP	48	0.11%	Titanium CP	2.86	0.0041	8.24	0.0118	Titanium CP	15.3
Titanium 6-4	54	0.11%	Titanium 6-4	3.52	0.0051	10.1	0.0146	Titanium 6-4	14.9
Cronidur 30	106	0.10%	Cronidur 30	30.4	0.0436	87.4	0.1256	Cronidur 30	10.3
Cronidur 30 Couples									
Inconel 625	133	0.66%	Inconel 625	6.49	0.0093	32.9	0.0472	Inconel 625	8.3
Hastelloy C276	123	0.62%	Hastelloy C276	7.56	0.0109	38.3	0.0550	Hastelloy C276	7.2
Titanium CP	68	0.87%	Titanium CP	7.52	0.0108	38.1	0.0547	Titanium CP	5.6
Titanium 6-4	59	0.88%	Titanium 6-4	7.58	0.0109	38.4	0.0552	Titanium 6-4	6.0
Titanium LI	60	0.98%	Titanium LI	7.65	0.0110	38.7	0.0556	Titanium LI	6.3

Open Galvanic
Potential

Analogous to 'corrosion rate'
for non-passivating metals

Includes recession
plus outward growth

Anodically aggressive
configurations stabilize quickly

Status and Results of Galvanic Testing

Galvanic Coupling Analysis for Alternate Brine Solution

Apparent Relative Nobility and Relative Corrosion Susceptibility			Oxidation Rates at Steady State Apparent Rates for Corrosion-Recession & Oxidation Activity				Stabilization Period Time To Reach ~90% Equilibrium		
Brine	Steady State Potential (mV _{AgCl})	Relative Susceptibility to Corrosion	Brine	Metal Recession		Anodic Oxide Growth		Brine	Induction Period (hours)
				(Å/day)	(mil/year)	(Å/day)	(mil/year)		
Inconel 625 Couples									
Hastelloy C276	170	0.53%	Hastelloy C276	3.57	0.0051	18.8	0.0271	Hastelloy C276	15.3
Titanium CP	144	0.57%	Titanium CP	7.62	0.0109	40.1	0.0577	Titanium CP	3.6
Titanium 6-4	92	0.76%	Titanium 6-4	9.41	0.0135	49.6	0.0712	Titanium 6-4	4.6
Titanium LI	81	0.77%	Titanium LI	7.31	0.0105	38.5	0.0554	Titanium LI	4.2
Cronidur 30	122	0.68%	Cronidur 30	3.03	0.0043	15.9	0.0229	Cronidur 30	10.7
Hastelloy C276 Couples									
Inconel 625	183	0.54%	Inconel 625	3.18	0.0046	15.7	0.0225	Inconel 625	14.8
Titanium CP	175	0.57%	Titanium CP	8.74	0.0126	43.0	0.0618	Titanium CP	5.6
Titanium 6-4	143	0.67%	Titanium 6-4	8.57	0.0123	42.2	0.0606	Titanium 6-4	6.3
Titanium LI	132	0.71%	Titanium LI	8.31	0.0119	40.9	0.0588	Titanium LI	5.6
Cronidur 30	122	0.65%	Cronidur 30	2.98	0.0043	14.7	0.0211	Cronidur 30	7.7
Titanium CP Couples									
Inconel 625	104	0.03%	Inconel 625	29.5	0.0424	76.9	0.1105	Inconel 625	6.9
Hastelloy C276	131	0.03%	Hastelloy C276	27.6	0.0396	71.8	0.1032	Hastelloy C276	10.4
Titanium 6-4	27	0.05%	Titanium 6-4	2.93	0.0042	9.34	0.0110	Titanium 6-4	19.5
Titanium LI	29	0.04%	Titanium LI	3.15	0.0045	8.19	0.0118	Titanium LI	19.1
Cronidur 30	105	0.03%	Cronidur 30	35.6	0.0512	92.7	0.1333	Cronidur 30	10.5
Titanium 6-4 Couples									
Inconel 625	134	0.08%	Inconel 625	42.2	0.0607	122	0.1751	Inconel 625	8.5
Hastelloy C276	100	0.10%	Hastelloy C276	40.8	0.0587	118	0.1693	Hastelloy C276	10.9
Titanium CP	23	0.13%	Titanium CP	3.51	0.0050	10.12	0.0145	Titanium CP	19.2
Titanium LI	34	0.12%	Titanium LI	2.61	0.0037	7.52	0.0108	Titanium LI	18.1
Cronidur 30	104	0.09%	Cronidur 30	39.1	0.0561	112.7	0.1619	Cronidur 30	12.2
Titanium LI Couples									
Inconel 625	123	0.09%	Inconel 625	26.8	0.0385	77.1	0.1109	Inconel 625	8.2
Hastelloy C276	89	0.11%	Hastelloy C276	33.1	0.0475	95.2	0.1368	Hastelloy C276	10.7
Titanium CP	26	0.13%	Titanium CP	2.63	0.0038	7.58	0.0109	Titanium CP	19.5
Titanium 6-4	37	0.12%	Titanium 6-4	2.79	0.0040	8.05	0.0116	Titanium 6-4	18.2
Cronidur 30	79	0.10%	Cronidur 30	38.9	0.0560	112	0.1611	Cronidur 30	11.1
Cronidur 30 Couples									
Inconel 625	140	0.58%	Inconel 625	6.80	0.0098	34.4	0.0495	Inconel 625	10.2
Hastelloy C276	104	0.74%	Hastelloy C276	6.22	0.0089	31.5	0.0452	Hastelloy C276	7.4
Titanium CP	62	0.88%	Titanium CP	7.18	0.0103	36.4	0.0523	Titanium CP	6.3
Titanium 6-4	59	0.86%	Titanium 6-4	7.94	0.0114	40.2	0.0578	Titanium 6-4	7.0
Titanium LI	120	0.69%	Titanium LI	9.71	0.0139	49.1	0.0706	Titanium LI	6.7

Open Galvanic
Potential

Analogous to 'corrosion rate'
for non-passivating metals

Includes recession
plus outward growth

Anodically aggressive
configurations stabilize quickly

Status and Results of Galvanic Testing

Galvanic Compatibility Rankings for Independent Coupling

Couple Pair ↔	Potential Difference		Corrosion Susceptibility		Metal Recession Rate		Oxidation/Dissolution Rate		Stabilization Period	
	Differential (mV _{AgCl})	Deviation (%)	Differential (ppm)	Deviation (%)	Differential (Å/day)	Deviation (%)	Differential (Å/day)	Deviation (%)	Differential (hours)	Deviation (%)

Pretreat Solution

For all fields, the smaller the value, the greater the apparent compatibility between the two metals.

Ti64/TiLI ↔ TiLI/Ti64	3.50	6.33%	0.052	0.47%	0.221	6.48%	0.619	6.30%	0.100	0.67%
TiLI/TiCP ↔ TiCP/TiLI	4.33	8.58%	7.52	101%	0.569	18.1%	0.691	8.05%	0.183	1.21%
TiCP/Ti64 ↔ Ti64/TiCP	4.57	8.66%	7.23	98.5%	0.516	18.3%	0.624	8.11%	0.251	1.70%
Inco/Hast ↔ Hast/Inco	20.2	14.7%	0.39	0.65%	0.420	13.9%	3.19	20.6%	0.460	3.75%
Cron/Inco ↔ Inco/Cron	23.3	19.3%	1.03	1.55%	3.90	86.0%	19.2	82.7%	0.315	3.86%
Hast/Cron ↔ Cron/Hast	24.5	18.2%	1.16	1.90%	4.35	80.8%	22.5	83.1%	0.345	4.90%
TiCP/Cron ↔ Cron/TiCP	42.3	47.3%	82.6	182%	25.5	126%	48.0	77.3%	4.18	54.6%
TiLI/Hast ↔ Hast/TiLI	43.7	47.4%	70.5	160%	32.2	126%	73.3	87.6%	4.81	65.8%
Ti64/Inco ↔ Inco/Ti64	43.9	42.5%	62.6	157%	35.6	130%	80.1	88.9%	3.64	61.8%
Ti64/Cron ↔ Cron/Ti64	44.0	54.1%	79.0	162%	24.0	123%	52.8	81.5%	4.16	51.2%
Ti64/Hast ↔ Hast/Ti64	45.7	46.0%	67.8	159%	26.6	129%	61.8	92.7%	3.74	58.4%
TiLI/Cron ↔ Cron/TiLI	45.8	55.3%	87.7	163%	22.7	120%	48.7	77.2%	4.05	48.9%
TiCP/Hast ↔ Hast/TiCP	47.7	56.0%	80.3	186%	25.5	136%	52.3	93.9%	3.70	60.1%
TiCP/Inco ↔ Inco/TiCP	48.2	47.0%	69.9	185%	33.9	139%	68.4	93.1%	3.61	65.0%
TiLI/Inco ↔ Inco/TiLI	49.8	50.1%	64.8	159%	35.6	134%	81.9	94.4%	3.90	61.4%

Brine Solution

For all fields, the smaller the value, the greater the apparent compatibility between the two metals.

Ti64/TiLI ↔ TiLI/Ti64	2.82	7.92%	0.077	0.65%	0.186	6.90%	0.523	6.72%	0.087	0.48%
TiCP/Ti64 ↔ Ti64/TiCP	3.33	13.3%	8.05	92.6%	0.578	18.0%	0.784	8.06%	0.250	1.29%
TiLI/TiCP ↔ TiCP/TiLI	3.70	13.5%	8.43	102%	0.513	17.7%	0.608	7.71%	0.350	1.82%
Inco/Hast ↔ Hast/Inco	13.7	7.74%	0.873	1.64%	0.389	11.5%	3.15	18.3%	0.477	3.17%
Hast/Cron ↔ Cron/Hast	17.2	15.2%	9.12	13.2%	3.24	70.3%	16.8	72.8%	0.283	3.73%
Cron/Inco ↔ Inco/Cron	18.5	14.1%	9.98	15.8%	3.77	76.8%	18.5	73.4%	0.427	4.08%
TiCP/Inco ↔ Inco/TiCP	40.0	32.3%	53.9	180%	21.9	118%	36.7	62.8%	3.33	63.0%
TiLI/Cron ↔ Cron/TiLI	41.0	41.2%	58.9	150%	29.2	120%	63.0	78.1%	4.46	50.2%
TiLI/Inco ↔ Inco/TiLI	41.5	40.7%	68.3	158%	19.5	114%	38.6	66.7%	3.93	63.4%
Ti64/Hast ↔ Hast/Ti64	42.7	35.2%	56.9	149%	32.3	131%	75.6	94.5%	4.64	53.9%
Ti64/Inco ↔ Inco/Ti64	42.8	37.9%	67.8	160%	32.8	127%	72.2	84.3%	3.93	59.9%
TiCP/Cron ↔ Cron/TiCP	43.0	51.8%	84.9	186%	28.4	133%	56.4	87.3%	4.23	50.3%
TiLI/Hast ↔ Hast/TiLI	43.0	39.0%	60.7	148%	24.8	120%	54.3	79.7%	5.10	62.6%
TiCP/Hast ↔ Hast/TiCP	43.8	28.6%	54.3	182%	18.9	104%	28.8	50.2%	4.87	60.8%
Ti64/Cron ↔ Cron/Ti64	45.2	55.4%	76.9	161%	31.1	132%	72.5	94.8%	5.21	54.4%

Status and Results of Galvanic Testing

Galvanic Compatibility Indications for Concurrent Coupling

Sum of the Differentials: Apparent compatibility indicated for each metal in the presence of all the other metals

Pretreat

	Potential Difference Σ Differentials (mV _{AgCl})	Corrosion Susceptibility Σ Differentials (ppm)	Recession Rate Σ Differentials (Å/day)	Passivation Rate Σ Differentials (Å/day)	Stabilization Period Σ Differentials (hours)	Passivation-Recession Ratio Protection Strength Index (PSI)
Titanium 64	141.6	216.6	92.61	195.9	11.89	2.116
Titanium CP	147.1	247.5	85.98	170.0	11.92	1.978
Titanium LI	147.2	230.5	91.37	205.2	13.05	2.245
Cronidur 30	180.0	251.5	80.53	191.2	13.05	2.374
Hastelloy C276	181.7	220.1	89.00	213.1	13.06	2.394
Inconel 625	185.5	198.7	109.5	252.8	11.92	2.309

Brine

	Potential Difference Σ Differentials (mV _{AgCl})	Corrosion Susceptibility Σ Differentials (ppm)	Recession Rate Σ Differentials (Å/day)	Passivation Rate Σ Differentials (Å/day)	Stabilization Period Σ Differentials (hours)	Passivation-Recession Ratio Protection Strength Index (PSI)
Titanium 64	132.0	196.4	74.16	157.0	13.93	2.117
Titanium CP	133.8	209.6	70.29	123.3	13.02	1.754
Titanium LI	136.8	209.7	96.95	221.6	14.03	2.286
Cronidur 30	156.5	200.9	78.36	169.2	12.10	2.159
Hastelloy C276	160.3	181.9	79.49	178.7	15.37	2.247
Inconel 625	164.8	239.8	95.8	227.1	14.61	2.371

Overall, the net compatibilities indicated for each metal while in the presence of the other five metals, appear to be similar. These differences are within the margins of error. In summary, each metal candidate appears to be compatible with all the other metals jointly and concurrently.

Metal Materials Compatibility Final Report

Summary of Key Points, Conclusions and Comments

Wedge/Sandwich Crevice Results

- Neither 6 month and 12 month ambient soaking of crevice samples indicated any visible signs of corrosion, etching, recession, pitting, crevicing, extraneous surface growth or base metal degradation in either solution. However . . .
- Surface discolorations developed on some of the samples during rinsing which appeared to be superficial aberrations confined within the oxide layer. XPS analysis did not indicate any compositional anomalies. The effects seemed to be most prominent on Titanium surfaces.
- From a corrosion perspective, these aberrations are considered to be inconsequential with no effects on base metal recession or the self-healing properties of the passivation oxide protection mechanism.

General Corrosion Results

- Open Circuit, Linear and Tafel polarization indicated extremely low general corrosion rates which were superior to an *outstanding* rating for all six metals in both solutions.
- In terms of *general* corrosion, relative nobility, low susceptibility and low recession rate, overall average ranking of the six metals can be divided into two basic metals groups . . .
Titanium CP, Titanium LI, Titanium 64 > Cronidur 30, Inconel 625, Hastelloy C276
- In terms of general corrosion rate activity in situations reflective of open circuit and slightly powered conditions, the pretreat solution appears to be about 2 ½ times more active than the brine solution, on the average. However . . .

Metal Materials Compatibility Final Report

Summary of Key Points, Conclusions and Comments

Pitting Corrosion Results from Polarization Testing

- During cyclic polarization and pitting analysis, the situation is almost reversed . . . overall average pitting rates in the brine solution appeared to be about 3 times more active than those in the pretreat solution for all six metals. This likely related to concentrated chloride content.
- Analysis indicated that Cronidur 30 had a substantially higher susceptibility the initiation and sustained growth of pits than any of the other metals, with long term pitting rates many times greater than those for Inconel or Hastelloy under hypothetical worst-case scenarios.
- On the average, the overall ranking of the candidates in terms of high pitting susceptibility and average pitting rate under harsh conditions could be suggested . . .

Cronidur 30 >> Hastelloy C276, Inconel 625 > Titanium 64, Titanium LI, Titanium CP

Supplemental Polarization Comments

- Disregarding the appearance of surface oxide discolorations, all the Ti candidates seemed to be almost immune to general corrosion, pitting, crevicing, extreme anodic (breakdown) voltages and negative cathodic stripping voltages under accelerated corrosive conditions.
- While likely irrelevant to most field situations, high Ni alloys such as Inconel and Hastelloy appear to be vulnerable to cathodic stripping under the influence of strong negative potentials which can result in undesirable alterations to the passive layer and etching of the base metal.
- The preceding results pertain to individual samples which were isolated from other materials. They are not necessarily reflective of mixed systems subject to possible galvanic interactions.

Metal Materials Compatibility Final Report

Summary of Key Points, Conclusions and Comments

Galvanic Coupling Compatibility Results

- As with the Open Circuit measurements, Galvanic Coupling is a very slow real-time process in which corrosion events or visible surface changes on these kinds of noble metals is rarely observed. In some cases, it can take > 10 days to physically reach a Steady State.
- In order to accommodate the large number of coupling tests required for this study, modelled curve fits were required on most data traces in order to determine steady state values.
- All the metals indicated similar compatibilities when compared collectively with the other metals. A specific ranking is not proposed. However, a simplified statement indicating the apparent nobility based on the differentials between potential levels could be given . . .

Titanium 64, Titanium CP, Titanium LI >~ Cronidur 30, Hastelloy C276, Inconel 625

- Again, as it was with the Open Circuit measurements, the Pretreat solution appears to be slightly more active than the Brine solution, indicating somewhat higher galvanic potentials, base metal recession rates and passivation thickness growth rates, on the average. Recession and thickness *growth* rates are also an indication of the associated *redox* reaction rates.
- In addition to elevated levels of chloride which is concentrated in the brine, differences in the two solutions are also likely due to a balance shift between activation-controlled and diffusion-controlled chemical reactivity in which the thicker, more viscous brine solution hinders the flow of reactants and products into and away from redox reaction sites.

Appendix and Supplementary Topics

- **Atypical Results from Polarization Testing**

Examples of Anomalies, Outliers and Extreme Test Conditions. Presents images and analysis of destructive and unusual effects observed during extreme polarization testing conditions.

- **Analytical Methods and Estimation Techniques**

Introduces special techniques for indicating base metal recession, protective oxide thickness growth rates, evolution of the electrical double layer, oxide breakdown, composition and repassivation factors, long term estimates for pitting depth and pitting rate, corrosion susceptibilities and corrosion probability factors.

- I. Refined Method for the Estimation of Recession and Oxidation Rates

- II. Special Method for Determination of Electron Exchange Equivalents

- III. Definition of the Pitting Protection Ratio and the Corrosion Recovery Ratio

- IV. Definition of Susceptibilities for Corrosion, Pitting Initiation and Sustainment

- V. Model Development for Pitting Rates and Penetration Depths Over Time

- **Description of Events Around the Breakdown Region**

Provides technical assessments of the passivation/oxidation process, structure/configuration, mechanisms, evolution and destruction of the passive layer preceding and during the breakdown point. Explores likely reactions associated with oxide growth and the roles of metal interstitials and oxygen vacancies during oxide formation/degradation with references to the Point Defect Model (MacDonald, et.al.).

Atypical Results from Polarization Testing

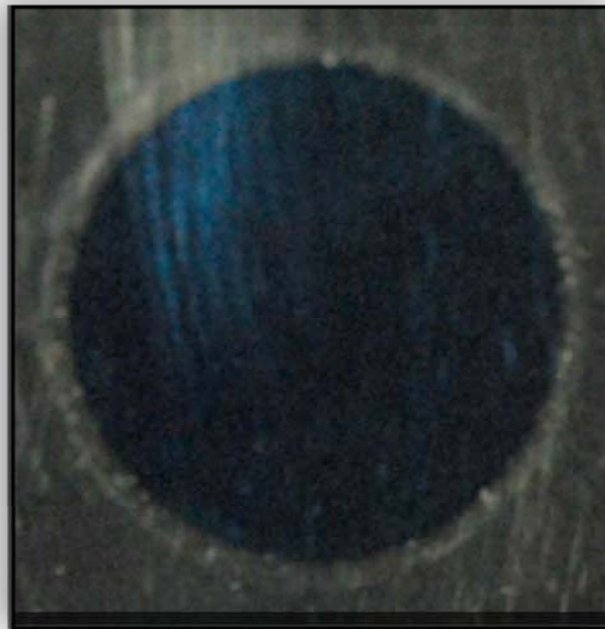
Examples of Anomalies, Outliers and Extreme Test Conditions

- In order to capture the breakdown region E_{Brk} , preselected cyclic polarization test parameters generally utilized reversal vertex points (E_{Ver}) of around 1.0-1.2 V for Inconel, Hastelloy and Cronidur, and 2.0-2.5 V for all the Titanium samples.
- Artifacts such as birefringent discolorations and powdery hydroxide precipitations sometimes developed while the test areas were being rinsed with DI water. The effects usually became more pronounced as the samples continued to dry in air. Several of the Titanium samples exhibited these superficial discolorations. However . . .

No pitting, etching or metal degradation was observed in any of the Titanium samples



Titanium LI in Pretreat – No unusual test conditions or results were noted; E_{Ver} was 2.2V; atypical in appearance (oxide aberrations)



Titanium 64 in Brine – No unusual test conditions or results were noted; E_{Ver} was 2.4V; atypical in appearance (oxide aberrations)



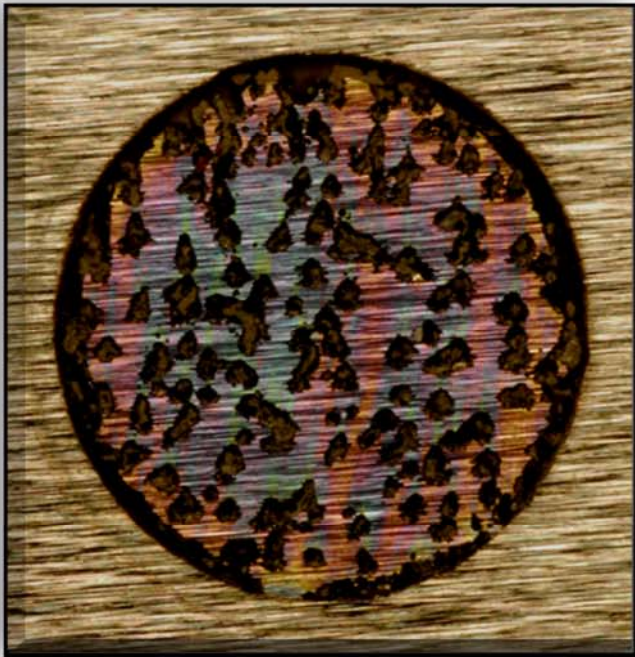
Titanium 64 in Brine – E_{Ver} was 4.1 V; appearance is typical of most Ti samples in spite of the unusually high vertex for this one

Atypical Results from Polarization Testing

Examples of Anomalies, Outliers and Extreme Test Conditions

- Intended potential reversal vertex points (E_{Ver}) were around 1.0-1.2 V for Inconel, Hastelloy and Cronidur, and 2.0-2.5 V for the all Titanium samples. Some of the samples were subjected to higher potentials . . . with destructive results.

Extreme voltages often lead to pitting and general etching of the base metal except for the Titanium alloys



Cronidur 30 in Pretreat – E_{Ver} was 10 V; accidental test over-run; extreme pitting and crevice damage is obvious; probably not practical for serious evaluation due to the excessive E_{Ver} .



Inconel 625 in Brine – E_{Ver} was 4.5 V; general etching into base metal (loss of oxide, loss of base metal); similar to the stripping effects noted in other peculiar test runs (next topic)



Titanium CP in Pretreat – E_{Ver} was 4.2 V; appearance typical of most Ti samples; no base metal damage on any of the Ti samples even when subjected to higher voltage

Atypical Results from Polarization Testing

Examples of Anomalies, Outliers and Extreme Test Conditions

- Generally, very negative values for E_{OC} and E_{Cor} imply native oxide layers which have been substantially altered by the solution. For high Ni alloys, low cathodic starting points during pretreat polarization testing appeared to impart a stripping effect on the oxide layer while a new, solution-formed oxide/hydroxide layer develops during the anodic branch of the test run.
- Stripping of air-formed passivation layers on Inconel and Hastelloy may begin as early as -0.2 V in the pretreat solution. The ‘stripping’ effect was not observed with any of the brine samples. Green $Ni(OH)_2$ subsequently forms on the affected surfaces during water rinse.

Cathodic conditioning in pretreat may promote corrosive degradation of Ni alloys



Inconel 625 in Pretreat – Starting potential was -0.5 V; significant etching (recession), hydroxide formation and possible plate-back of liberated Cr atoms onto base metal surface



Cronidur 30 in Pretreat – Starting potential was -0.75 V; other than some apparent crevicing near the o-ring, no etching, recession or large-scale oxide destruction was observed

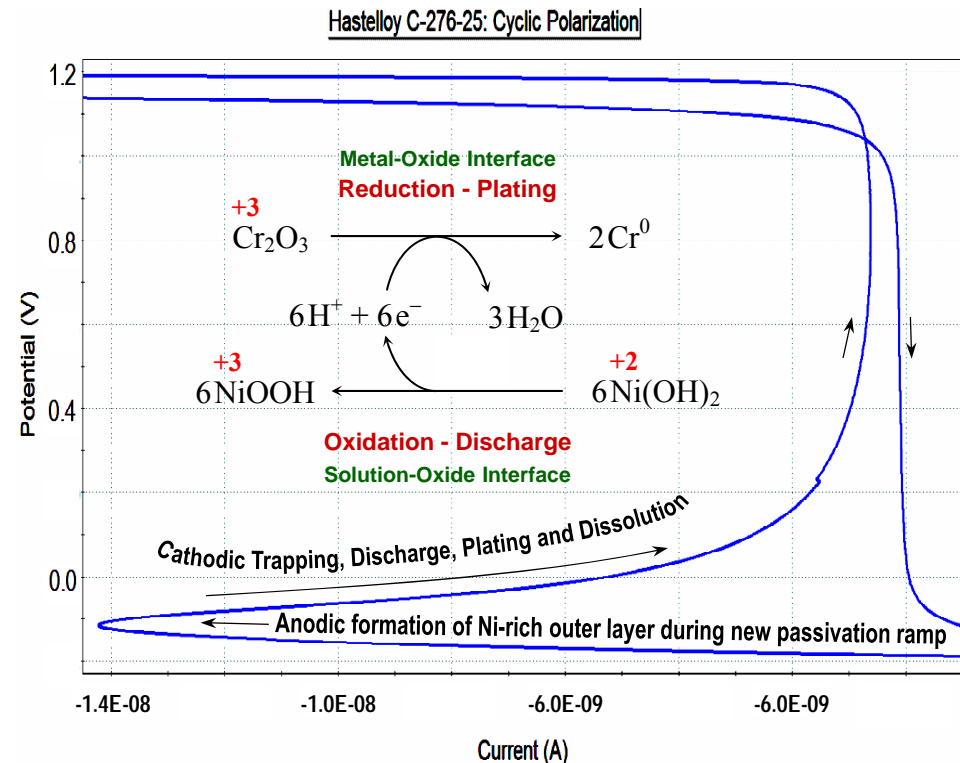
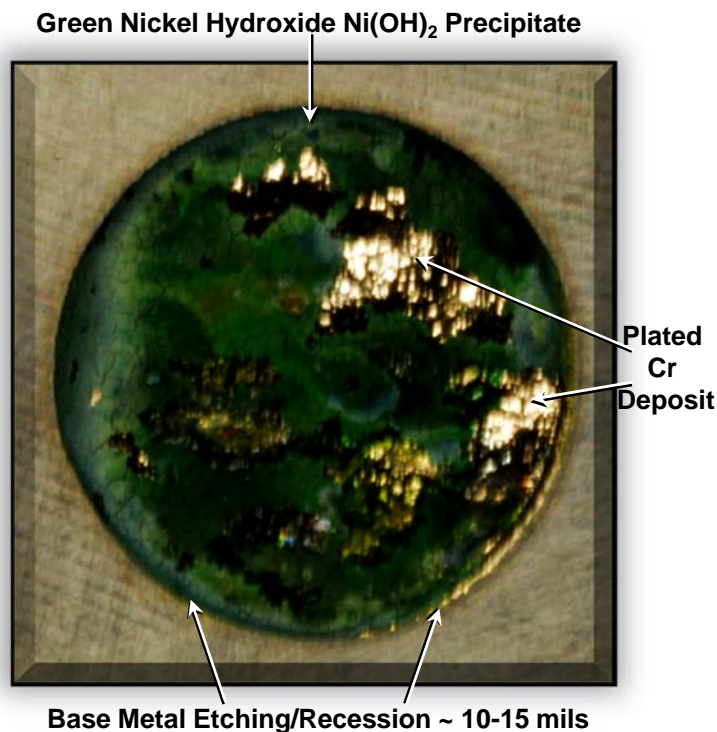


Titanium 64 in Pretreat – Starting potential was -0.75 V; no signs of any damage to the oxide or base metal were observed

Atypical Results from Polarization Testing

Exploring the Anomalous Cathodic Behavior in High Ni Alloys

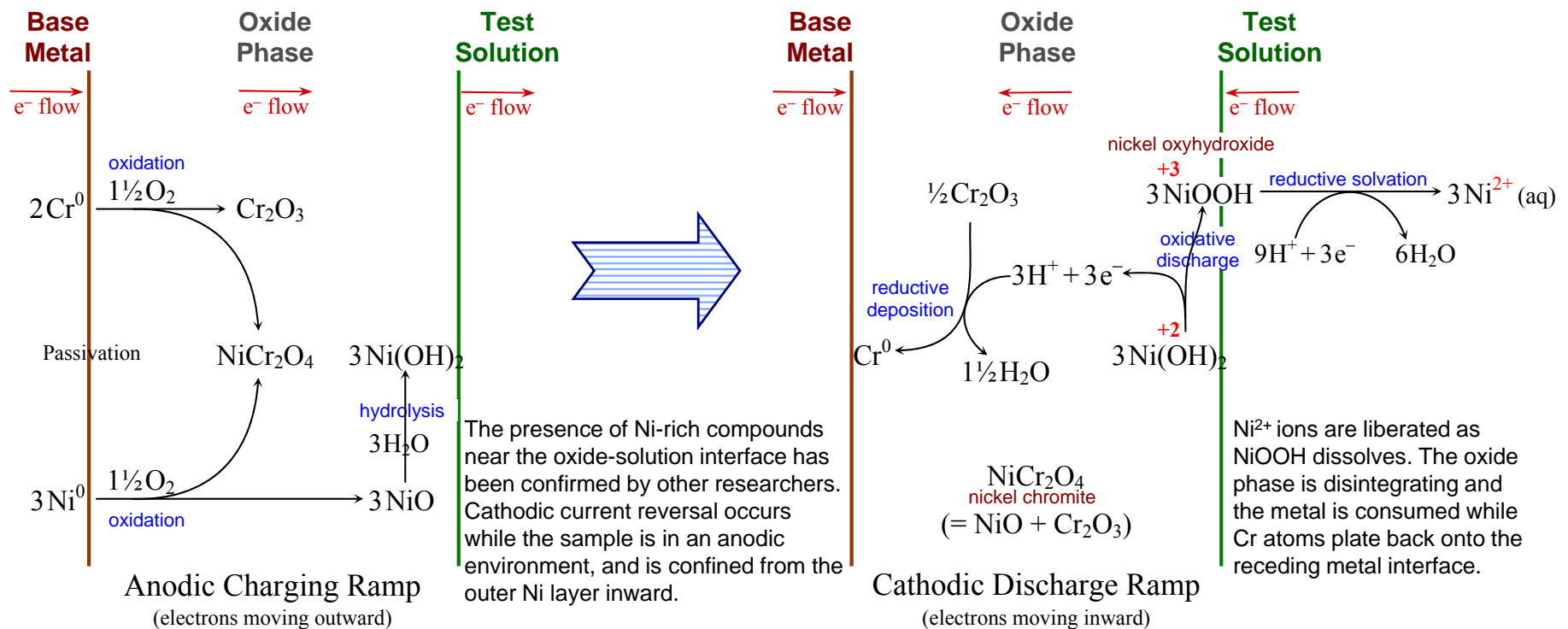
- It is proposed that cathodic stripping of the natural oxide layers on Inconel and Hastelloy leads to the subsequent formation of a Ni-rich oxide phase in which NiO forms and migrates to the outer oxide-solution interface in a bilayer configuration.
- Here, NiO acts as a barrier to current flow by ‘trapping’ electrons within the composite oxide layer which then leads to the reduction of Cr atoms near the metal interface along with ‘back-plating’ of Cr⁰ onto the base metal where a very thin, nonuniform layer of Cr⁰ is deposited.
- Peripheral NiO is converted into Ni(OH)₂ / NiOOH (much like a Ni-MH cell), however, the protective oxide/hydroxide layer dissolves, leading to substantial recession of the base metal.



Atypical Results from Polarization Testing

Mechanism for Cathodic Behavior During Passivation of High Ni Alloys

- During the initial passivation ramp, oxidation of Cr and Ni proceeds as usual to form Cr_2O_3 and NiO . It is suspected that nickel chromite NiCr_2O_4 comprises a substantial fraction of the oxide phase, just as iron chromite FeCr_2O_4 is expected to form in the outer passive layers of Cronidur and other stainless steels. Their roles during cathodic discharging are not exactly clear but they appear to provide enhanced pitting protection not seen with straight Cr_2O_3 .
- Near the solution interface, NiO is quickly hydrolyzed and then oxidized to the oxyhydroxide as the discharge effect commences. The outer $\text{NiO}/\text{Ni}(\text{OH})_2/\text{NiOOH}$ barrier layer 'traps' electrons within the oxide phase where the current direction reverses and the base metal becomes cathodic, leading to flash Cr deposition.

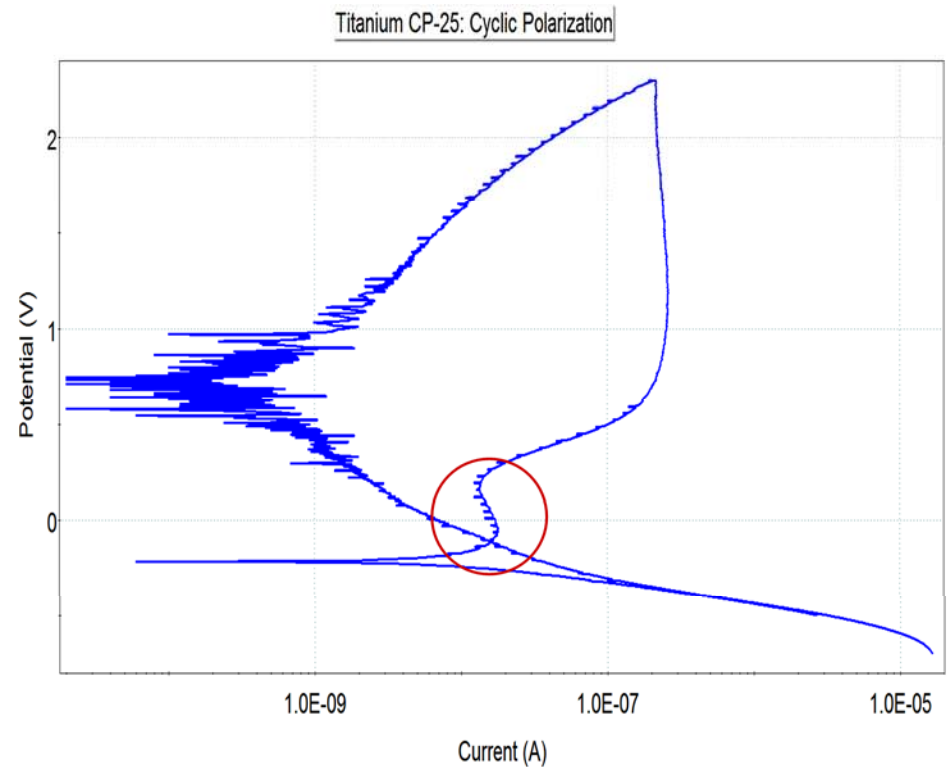
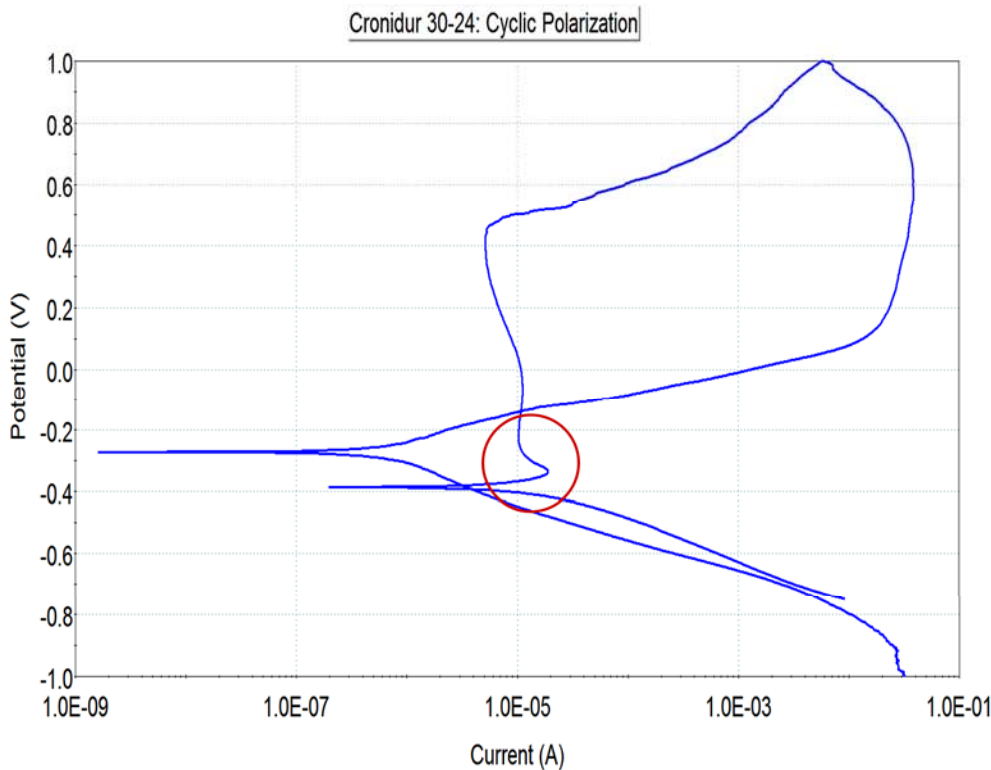


Atypical Results from Polarization Testing

Cathodic Trapping is Not Necessarily Limited to Ni Alloys

Outer layers rich in $\text{Fe}_x\text{O}_y/\text{FeOOH}$ and $\text{TiO}_2/\text{TiO}(\text{OH})_2$ may also exhibit effects similar to barrier/trapping in these solutions

Examples



Polarization results can be very sensitive – while a small degree of trapping may be indicated, neither of these samples visually showed any signs of general base metal etching/recession or general oxide degradation as was seen with the Ni alloys

I. Refined Method for the Estimation of Corrosion and Oxidation Rates (slide 1 of 2)

- The standard approach for generating approximations of corrosion rate is outlined in ASTM G102 using Faraday's law to provide results in units of "mils per year" (mil/year or mpy) from the measured current density . . .

$$k_{Cor} = C_1 W_{Eq} \left(\frac{I_{Cor}}{\rho_m} \right)$$

. . . where C_1 is a constant comprised of a combination of conversion terms equal to 128740 equivalents-seconds-mils / Coulombs-cm-years; W_{Eq} is the fractional equivalent weight of the alloy component (for a pure metal, W_{Eq} is simply the equivalent weight of the metal); I_{Cor} is the measured current density in Amps, and ρ_m is the fractional density of the alloy component (for a pure metal, ρ_m is simply the density of the metal). The factor can be modified to give Å/day.

- If polarization/corrosion *resistance* is the measured parameter, I_{Cor} can be given by

$$I_{Cor} = \frac{C_2}{R_{Cor}}$$

. . . which is an analogy to Ohm's law, where the constant C_2 may be a function of subsequent Tafel line slope analyses or developed/surmised by other means.

I. Refined Method for the Estimation of Corrosion and Oxidation Rates (slide 2 of 2)

- The following ideas are considered to be supplemental extensions to ASTM G102.
- For passive (anodic) oxide growth, an analogous concept can be proposed and utilized cautiously under certain conditions . . .

$$k_{Pas} = C_1 W_{Eq} \left(\frac{I_{Pas}}{\rho_{ox}} \right) = C_1 C_2 \frac{W_{Eq}}{\rho_{ox} R_{Pas}}$$

. . . where W_{Eq} is the fractional equivalent weight and ρ_{ox} is the fractional density of one of the oxide components. For a metal that generates a homogeneous passive layer, W_{Eq} and ρ_{ox} pertain to that oxide. However, for a passivation phase comprised of a mixture of oxides (as with most alloys), the net or composite sum of electron equivalents (and thus, equivalent weights) as well as the respective densities of each oxide component must be taken into account (see the section, Special Method for Determination of Electron Exchange Equivalents).

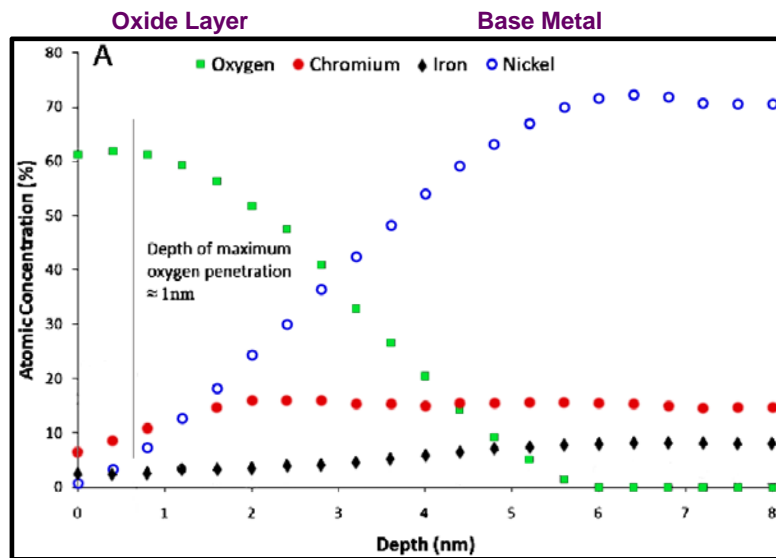
- With the appropriate modifications, similar expressions for pitting and repassivation can be written and utilized under certain conditions . . .

$$k_{Pit} = C_1 W_{Eq} \left(\frac{I_{Pit}}{\rho_m} \right) = C_1 C_2 \frac{W_{Eq}}{\rho_m R_{Pit}} \quad \text{and} \quad k_{ReP} = C_1 W_{Eq} \left(\frac{I_{ReP}}{\rho_{ox}} \right) = C_1 C_2 \frac{W_{Eq}}{\rho_{ox} R_{ReP}}$$

II. Special Method for Determination of Electron Exchange Equivalents (slide 1 of 3)

- Calculation of equivalent weights (W_{Eq}) for metals and alloys subjected to polarization measurements is required in order to determine corrosion/oxidation rates. Estimation of W_{Eq} values derived purely from base metal compositional ratios is common practice, but this not the best approach. ASTM G-102 mentions the concept of selective oxidation.
- In fact, there has been ample data published utilizing depth profiling via XPS (ESCA), SIMS and Auger analysis confirming that selective oxidation does indeed occur. Clearly, differences between metallic contents in base metal and the oxide layer are substantial.

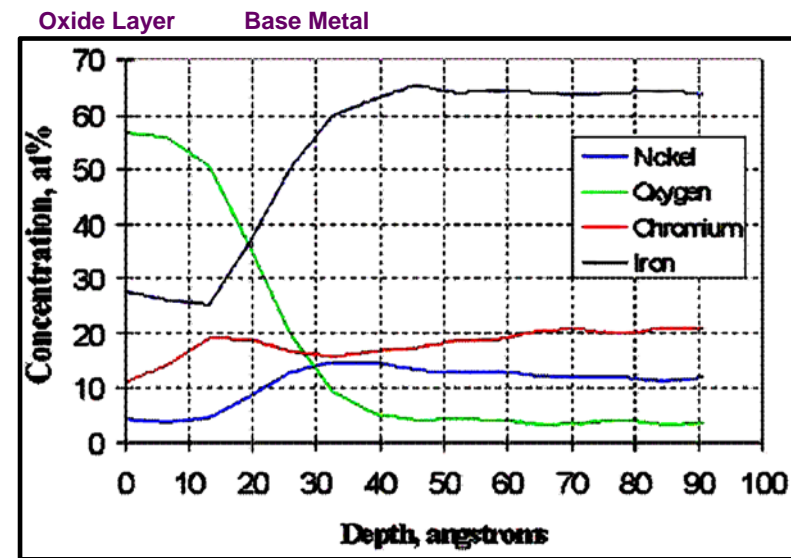
Examples



Inconel 700 passive oxide composition*

Typical base metal components:

Ni 46%, Cr 15%



SS 316 passive oxide composition**

Typical base metal components:

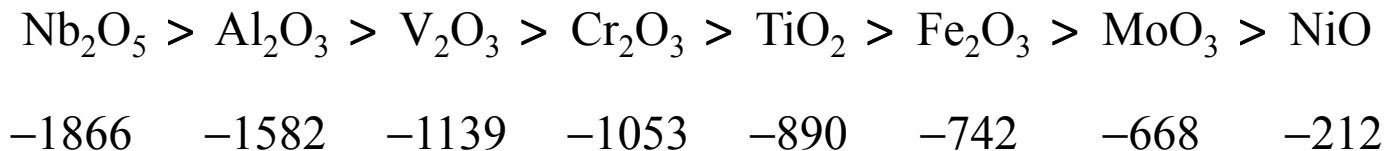
Fe 67%, Cr 17%, Ni 12%

* Passivation Oxide Controlled Selective Carbon Nanotube Growth on Metal Substrates, J B Bult, W G Sawyer, P M Ajayan and L S Schadler, Nanotechnology 20 (2009) 085302

**XPS Analysis of the Passivation Layer on Stainless Steel, Innovatech Labs, Plymouth, MN

II. Special Method for Determination of Electron Exchange Equivalents (slide 2 of 3)

- The following approach is proposed as an extension to ASTM G102.
- The number of equivalent electrons transferred from the base metal during corrosive oxidation must equal (exactly) the number of electrons transferred to produce the alloy oxide (in accordance with the conservation laws).
- Recognizing certain factors associated with the formation and composition of the oxidation product are key to estimating how many exchange electrons are actually generated.
- It is well known that the various metals in an alloy will oxidize at different rates according to their Gibbs free energy of formation. For example, Cr_2O_3 ($\Delta G_f = -1053$ kJ/mol) is 5 times more likely to form than NiO ($\Delta G_f = -212$ kJ/mol). The ΔG_f values clearly reflect this.
- Thus, we state that the Relative Ease of Oxide Formation according to ΔG_f can be tabulated and ordered as illustrated in the following example . . .



- At present, estimation of equivalent weights (W_{Eq}) via oxide formation is complex, tedious and time-consuming. Even with the aid of Pourbaix diagrams, certain assumptions must be made and errors are likely without due diligence, but it is the correct way to determine the number of electrons transferred during the metal recession / oxidation growth process.

II. Special Method for Determination of Electron Exchange Equivalents (slide 3 of 3)

➤ An example of one of the metals treated in this manner for our study is given here.

Hastelloy C276 **Base Metal** Wrought Composition, As-Received – In Air

	Raw Wt%	Est Wt%	Mol. Wt.	Atomic %	# Eq. e ⁻	N _A e ⁻ /g
Ni	58.9%	59.3%	58.69	63.1%	0.67	1.14E-02
Cr	16.1%	16.2%	52.00	19.5%	2.72	5.24E-02
Mo	15.3%	15.4%	95.94	10.0%	0.55	5.75E-03
Fe	5.6%	5.6%	55.85	6.3%	0.39	6.92E-03
W	3.4%	3.4%	183.84	1.2%	0.10	5.18E-04
						Base Metal Net Equivalents
99.3%		100.0%	100.0%		4.42	13.0 g/mol
						Net Equivalent Weight
Density	8.89 g/cc		8.77 g/cc			
	measured		estimated			

Hastelloy C276 **Composite Oxide** Composition – In Acidic Test Solution

	Mole %	Atomic %	Less H ₂ O	# Eq. e ⁻	N _A e ⁻ /g
Cr ₂ O ₃	32%	Cr 21%	23%	2.031	1.34E-02
CrO ₃	8.9%			0.558	5.58E-03
CrOOH	0.48%			0.015	1.79E-04
CrOOH ₂ ⁺	3.7%			0.118	1.37E-03
NiO	10.5%	Ni 6.8%	7.2%	0.221	2.96E-03
Ni ₂ O ₃	4.1%			0.259	1.57E-03
NiOOH	0.60%			0.019	2.06E-04
NiOOH ₂ ⁺	5.3%			0.168	1.82E-03
MoO ₃	6.6%	Mo 2.5%	2.6%	0.416	2.89E-03
MoO ₂	0.53%			0.022	1.73E-04
MoO ₂ (OH) ₂	0.20%			0.012	7.70E-05
MoO(OH) ₃ ⁺	1.6%			0.102	6.24E-04
Fe ₂ O ₃	4.6%	Fe 3.5%	3.7%	0.289	1.81E-03
FeO	0.08%			0.002	2.28E-05
Fe ₃ O ₄	0.94%			0.074	3.20E-04
FeOOH	0.08%			0.002	2.68E-05
FeOOH ₂ ⁺	0.60%			0.019	2.11E-04
WO ₂	0.61%	W 0.47%	0.50%	0.026	1.18E-04
WO ₃	0.87%			0.055	2.37E-04
WO ₂ (OH) ₂	0.03%			0.002	6.59E-06
WO(OH) ₃ ⁺	0.21%			0.013	5.25E-05
4.42 Total Metal Equivalents					
H ₂ O	17%	O 65%	63%		
4.42 Total Oxygen Equivalents					
100.00%		100.00%	100.00%	29.8 g/mol	
Net Equivalent Weight					
4.00 g/cc					
theoretical density					

- Note the total electron equivalents is identical for the proposed oxide mixture *and* the original base alloy.
- The atomic concentrations in the oxide mixture are compliant with expectations via XPS, Auger, etc...
- Using only base metal compositions and typical valence electron equivalents, traditional estimates of W_{Eq} for this metal are on the order of 23-25g/mol.
- The W_{Eq} for the composite oxide developed from this approach can then be used to derive oxide growth information that is specific and unique to this alloy.

III. Definition of the Pitting Protection Ratio and the Corrosion Recovery Ratio (slide 1 of 3)

- When the oxide layer on a self-passivating metal is breached, it will attempt to heal or repair itself by quickly repassivating. The rate at which this rebuilding process occurs has a very strong influence on the net pitting protection afforded by the metal's natural oxide.
- During a typical cyclic polarization test run, information regarding general corrosion, pitting corrosion, passivation and repassivation are acquired. As an extension to the more traditional methods for evaluating polarization data, the following concepts were defined and utilized throughout this study. First, consider the Pitting Protection Ratio, PPR .
- PPR indicates how well the metal might 'protect' itself via localized repassivation/repair after the oxide has been compromised and pitting has initiated. It is given simply as the ratio of the maximum apparent current realized (I_{Pit}) following the breakdown potential (E_{Brk}) to the maximum apparent repassivation current realized (I_{ReP}) following the vertex (E_{Ver}) . . .

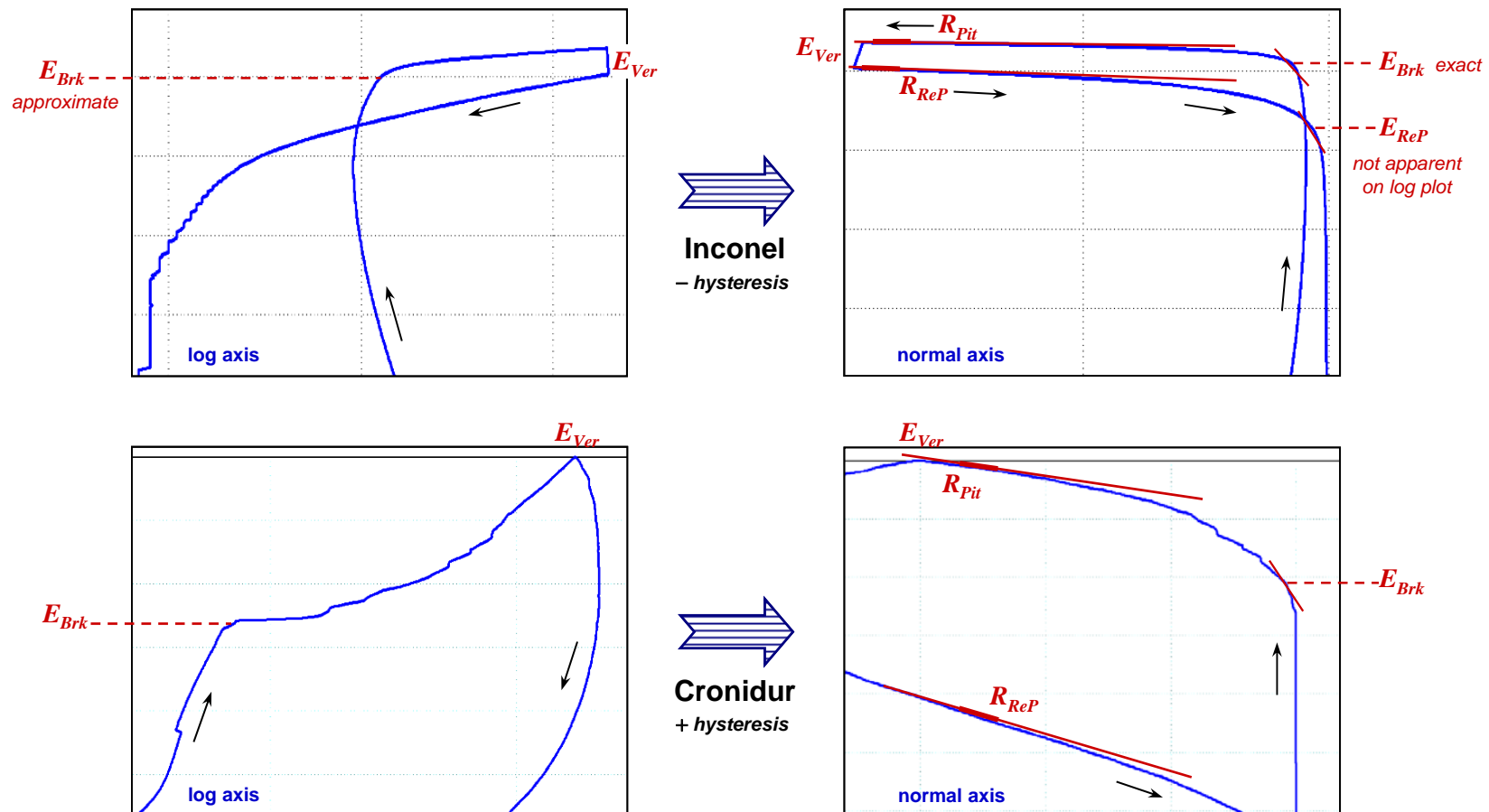
$$PPR = \frac{I_{Pit}}{I_{ReP}}$$

. . . where I_{Pit} is a direct measure of the maximum possible pitting rate achieved after E_{Brk} , and I_{ReP} directly measures the maximum possible repassivation rate after E_{Ver} , that is . . . $PPR = k_{Pit}/k_{ReP}$

- When $PPR > 1$, pitting is possible as the pitting rate overrides the repassivation rate. When $PPR < 1$, the metal is protected as any pits which might form are inhibited by rapid new oxide growth. In the event that $PPR = 1$, metastable pitting is implied. For PPR values $\ll 1$, pitting is highly improbable (as indicated from the titanium candidates in this study).

III. Definition of the Pitting Protection Ratio and the Corrosion Recovery Ratio (slide 2 of 3)

- The *PPR* method: Using both the normal and log plots, I_{Pit} and I_{ReP} are evaluated in the upper region of the cyclic curve associated with E_{Brk} and are given as $I_{Pit} = E_{Brk}/R_{Pit}$ and $I_{ReP} = E_{Brk}/R_{ReP}$ respectively, where R is the measured slope along the appropriate linear segments. The lowest slopes available in these regions represent the maximum rates. Much of the data extracted from cyclic curves in this study were obtained from the normal plots which often provide more discernable values than the traditional log plots. The following illustrations give examples for two of the *PPR* measurements processed in this study.



III. Definition of the Pitting Protection Ratio and the Corrosion Recovery Ratio (slide 3 of 3)

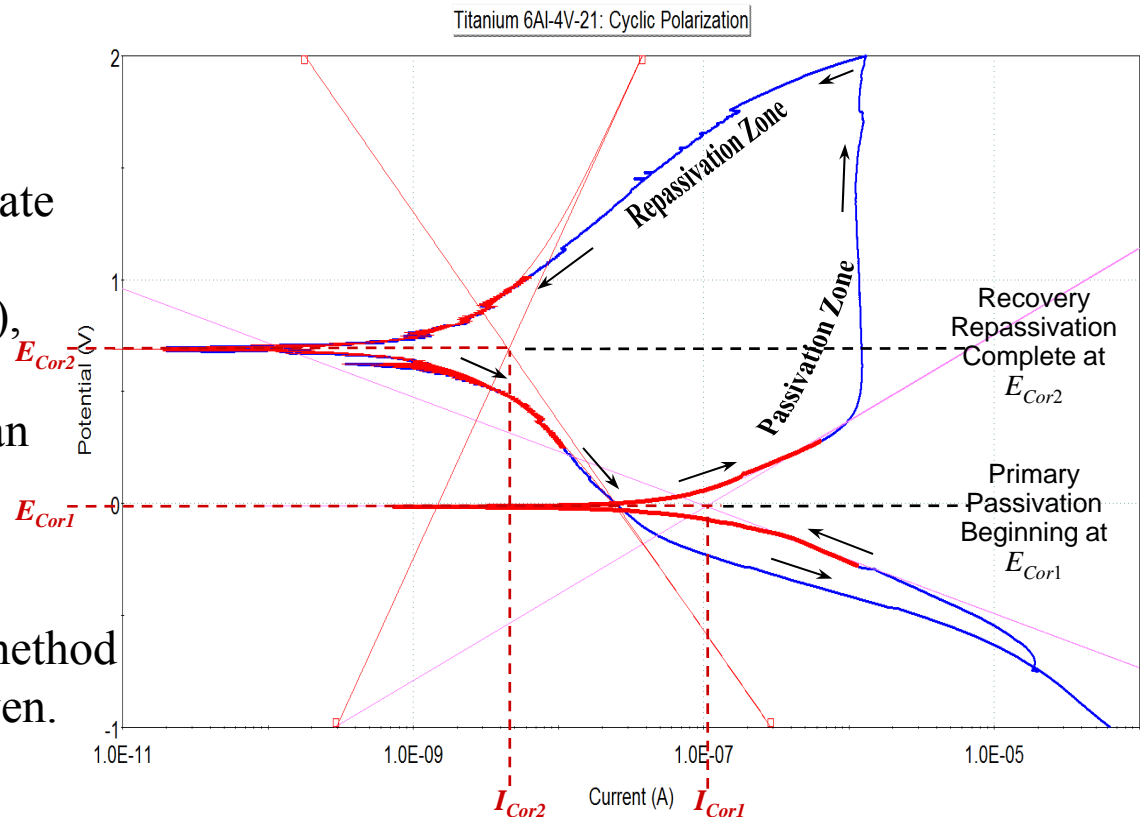
- During a cyclic polarization test, the Corrosion Recovery Ratio, CRR is given simply as the ratio of the corrosion rate at E_{Cor1} (the primary corrosion inflection point) represented as I_{Cor1} to the corrosion rate at E_{Cor2} (the secondary or *recovery* inflection point after repassivation is complete), represented as I_{Cor2} . That is . . .

$$CRR = \frac{I_{Cor1}}{I_{Cor2}}$$

- The CCR indicates how well the metal might 'recover' via general repassivation/repair after the oxide has been compromised and general corrosion has initiated.

- All the metals in this study indicate reduced corrosion rates after repassivation (lower I_{Cor2} values), inferring that the newly formed oxide phase is actually *better* than the original passivation layer (analogous to anodizing).

- An example showing the CCR method via standard Tafel analysis is given.



IV. Definition of Susceptibilities for Corrosion, Pitting Initiation and Sustainment (slide 1 of 4)

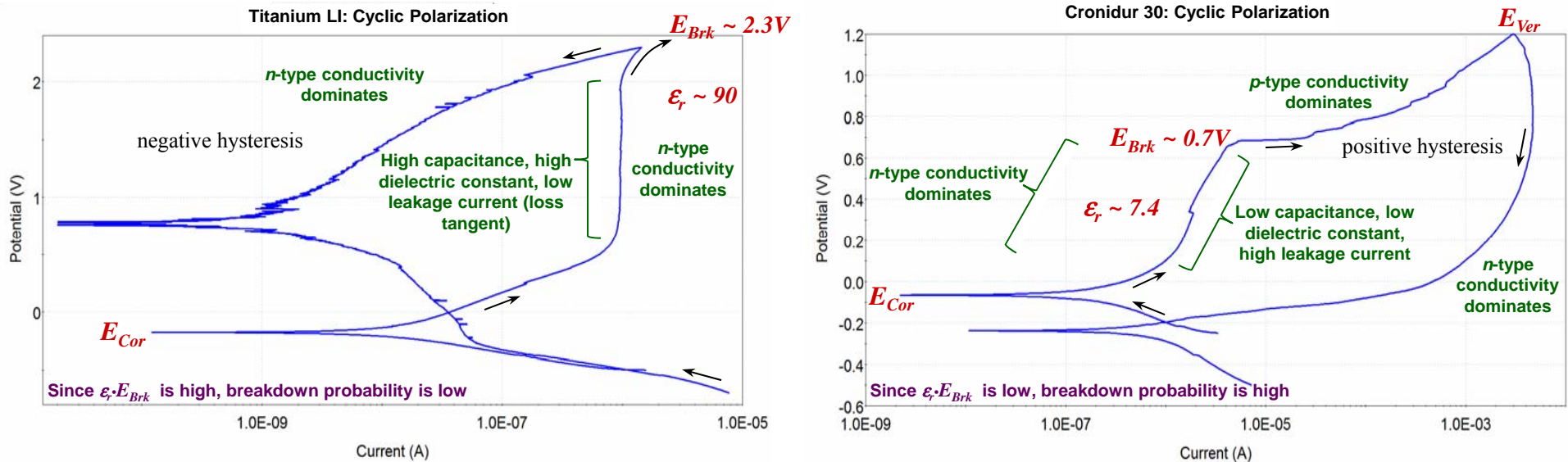
- Generally, the oxides studied here are all dielectrics exhibiting n -type semiconductivity with Cr^{3+} (or Ti^{4+}) interstitials as the donors which transition into p -type lattices at higher voltages near the breakdown potential E_{Brk} , where vacancies are created and Cr^{3+} cations are ejected.
- During polarization, the dielectric oxide layer evolves in thickness and composition along with analogous changes in pseudocapacitance $C = q/E_{App} = \epsilon_0\epsilon_r A/t$, surface charge density $\sigma = q/A = \epsilon_0\epsilon_r E_{App}/t$ and electric field strength $\mathcal{E}_{Pol} = \sigma/\epsilon$ (in accordance with Gauss' law).
 . . . where q is the charge transferred from the base metal to the oxide to the solution, E_{App} is the applied test voltage (the potential difference across the oxide), A is the sample test area (1 cm^2), t is roughly the oxide thickness, ϵ_0 is the vacuum permittivity constant, ϵ_r is the relative permittivity of the oxide (that is, ϵ_r is the dielectric constant of the oxide while $\epsilon_0\epsilon_r = \epsilon$ is the absolute permittivity of the oxide).
- Now it is recognized that $\mathcal{E}_{Pol} = \sigma/\epsilon = CE_{App}/A\epsilon$, or . . . $\mathcal{E}_{Pol}\epsilon = CE_{App}t/A$ from which a representative dielectric 'quality factor' or 'strength indicator' specific to that oxide layer can be envisioned. That is, at the breakdown point, it is suggested that . . .

$$E_{Brk}\epsilon_r \approx \text{constant}$$

- This implies that the product of the breakdown potential and the dielectric constant carries a special significance regarding the strength of the oxide layer and its relationship to corrosive tendencies. It is important to note that the probability that breakdown will occur is inversely related to both E_{Brk} and ϵ_r . One factor can compensate for the other. That is, if a given layer has a relatively low ϵ_r but a high E_{Brk} , it can still exhibit a low breakdown probability, and vice versa. If both factors are small, the probability is high, oxide failure is imminent and subsequent pitting is possible. These insights are consistent with real world perceptions.

IV. Definition of Susceptibilities for Corrosion, Pitting Initiation and Sustainment (slide 2 of 4)

- Consider two contrasting cases taken from typical Titanium and Cronidur cyclic runs:



- Just after the current changes from cathodic to anodic at E_{Cor} , the oxide layer rapidly develops. When most of the growth is complete, the curve passes into the semiconductive zone as the slope rapidly increases while q and C increase. During this plateau, base metal interstitials pass into the oxide phase which densifies, exhibiting n -type semiconductivity.
- Just before E_{Brk} , metal cations pass into the solution (p -type conductivity) as q discharges and the oxide begins to weaken. After E_{Ver} , the oxide rapidly rebuilds itself as base metal interstitials continue to participate in the production of oxide (n -type conductivity).
- It is inferred here that the oxide layer on the titanium sample possess an extremely low probability of breakdown/failure, while the oxide layer on the Cronidur sample is many times more susceptible. In general, titanium and its alloys exhibit high values for both E_{Brk} and ϵ_r and are well known for their nobility to surface-related corrosion phenomena.

IV. Definition of Susceptibilities for Corrosion, Pitting Initiation and Sustainment (slide 3 of 4)

- From another perspective, it is recognized that the greater the potential difference between E_{Brk} and the primary passivation potential, $\Delta E = E_{Brk} - E_{Pas}$, the lower the probability that pits will initiate, while the smaller the difference between E_{Brk} and the repassivation potential, $\Delta E = E_{Brk} - E_{ReP}$, the lower the probability that pits will continue to grow.
- As an extension to the more traditional methods for evaluating polarization data, the following concepts have been defined and utilized in this study. It is suggested that relative susceptibilities for the *initiation* (nucleation) and *sustainment* (unabated growth) of pitting can be represented respectively by the following arguments . . .

$$\left(\frac{E_{Brk} - E_{Pas}}{\epsilon_r E_{Brk}} \right) \quad \text{and} \quad \left(\frac{E_{Brk} - E_{ReP}}{\epsilon_r E_{Brk}} \right)$$

- Formal definitions can then be proposed for the relative susceptibilities to Pitting Initiation S_{PiI} and Pitting Sustainment S_{PiS} in fractional form, respectively . . .

$$S_{PiI} = 1 - \exp \left[- \left(\frac{E_{Brk} - E_{Pas}}{\epsilon_r E_{Brk}} \right)^{-1} \right] \quad \text{and} \quad S_{PiS} = 1 - \exp \left[- \left(\frac{E_{Brk} - E_{ReP}}{\epsilon_r E_{Brk}} \right) \right]$$

- When S_{PiI} is high, E_{Brk} and E_{Pas} are close together, and when S_{PiS} is high, E_{Brk} and E_{ReP} are far apart. This is in accordance with recognized interpretations of cyclic polarization curves.

IV. Definition of Susceptibilities for Corrosion, Pitting Initiation and Sustainment (slide 3 of 4)

- In an analogous approach, the following expression could also be suggested regarding the Susceptibility for General Corrosion for positive values of E_{OCP} and/or E_{Cor} . . .

$$S_{Cor} = 1 - \exp \left[- \left(\frac{E_{Cor} - E_f^0}{\epsilon_r E_f^0} \right)^{-1} \right]$$

. . . where E_f^0 is the estimated standard electrode potential associated with the Gibbs free energy of formation for each composite oxide in accordance with Nernst's equation . . . $\Delta G_f^0 = -nFE_f^0$. A large table of ΔG_f values was developed during this study defining each of the oxide components relevant to the metals under investigation (see Special Method for Determination of Electron Exchange Equivalents).

- Likewise, the probability that general corrosion will occur decreases as the difference $E_{Cor} - E_f^0$ increases and as the product $\epsilon_r \cdot E_f^0$ decreases. Estimated average values assimilated for ϵ_r and E_f^0 and utilized in this study are given in the following table . . .

	Inconel 625	Hastelloy C-276	Titanium CP	Titanium 6Al-4V	Titanium LI	Cronidur 30
ϵ_r	12.5	11.4	110	90.2	90.4	7.38
E_f^0	22.6 mV	22.0 mV	9.57 mV	20.4 mV	20.3 mV	15.3 mV

Note: Although native 'ambient' averages for ϵ_r have been utilized in this study, the value of ϵ_r can vary slightly as the oxide adapts to the test environment. Thus, for the time being, the susceptibilities presented in this report are best considered to be 'relative' until the methodology is further refined. Improved values for ϵ_r in specific test environments can be obtained via Electrochemical Impedance Spectroscopy (EIS) which will be pursued in future studies.

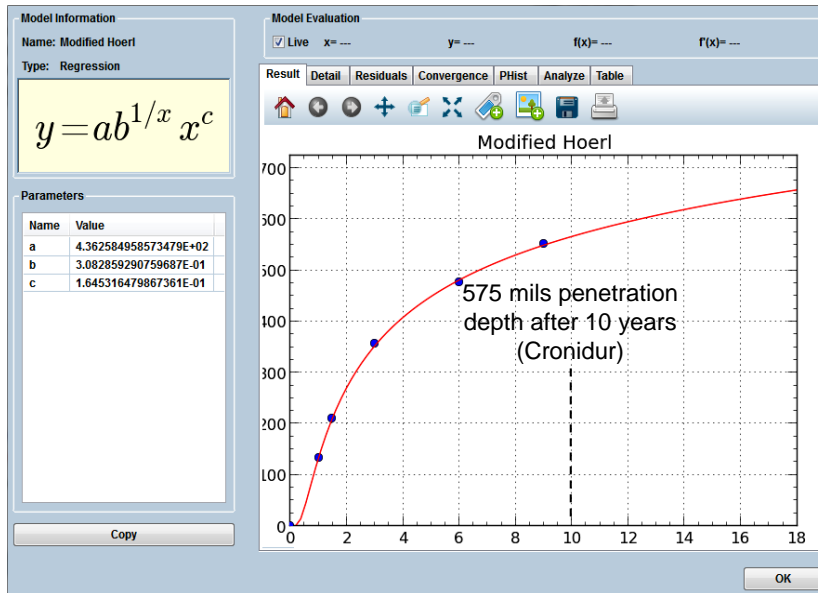
V. Model Development for Pitting Rates and Penetration Depths Over Time (slide 1 of 4)

- While general corrosion rates appeared to be higher in the Pretreat environment, pitting susceptibilities seemed to be more prominent in the Brine test solutions. This may be due to the concentrated chloride content in the Brine media.
- However, under normal operating conditions, it is believed that pitting is extremely unlikely in either solution with any of these metal candidates, including Cronidur.
- The observed pitting on Cronidur samples during polarization testing occurred under aggressive/accelerated test conditions where higher voltages were applied at rapid rates.
- While small voltages may simulate accelerated life conditions to a degree, higher voltages tend to promote side reactions, degradation effects and anomalies that would not occur under normal conditions and are not associated with the corrosion process.
- Caution must be exercised when interpreting data from the upper anodic regions of polarization curves, particularly the maximum pitting and repassivation rates.
- In the rare event that sustained pitting growth continued to progress into one of the subject metals, these tools may help provide some insight regarding long term pitting rates and pitting depths under hypothetical *worst-case scenarios*. At present, such projections are academic and are given primarily for informational purposes.

V. Model Development for Pitting Rates and Penetration Depths Over Time (slide 2 of 4)

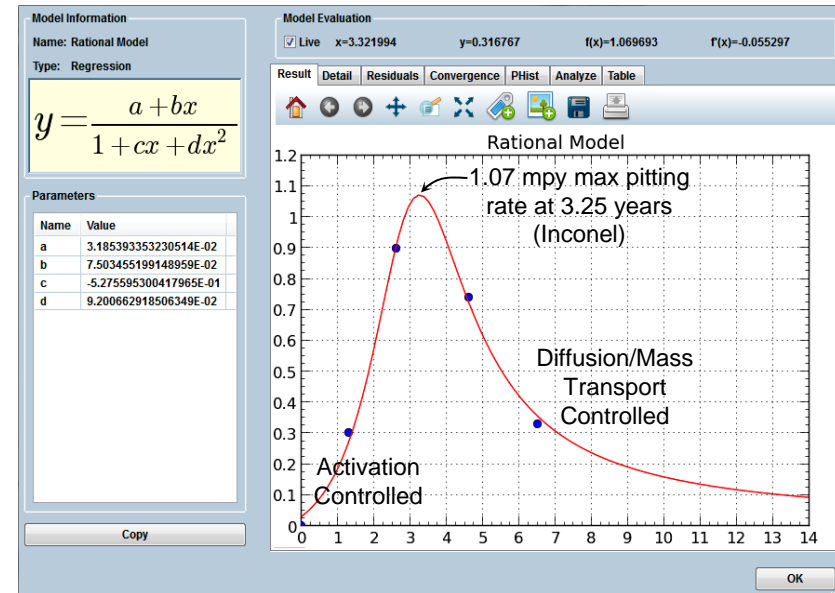
- Utilizing measured pitting depths published within the literature for Inconel 600 and 304 Stainless Steel in oceanic seawater gathered over several years, characteristic *curve forms* for pitting depth and pitting rate over time were recognized and established.
- Taking into account solution differences (pH, Cl⁻ content, temperature) and utilizing specific polarization data and analysis developed for the metal candidates in this study, model curves were developed for each of the six materials in both the pretreat and brine solutions. A couple of examples of these fits and results are given below.

Cronidur 30 Pitting Depth in Brine



Pitting depth ultimately reaches a maximum as the rate eventually subsides

Inconel 625 Pitting Rate in Pretreat



Pitting rate tapers off and eventually subsides when repassivation finally takes over

Status and Results of Polarization Testing (slide 3 of 4)

Model Pitting Rates and Pitting Depths for Worst Case Scenario

Ranked from lowest Pitting Depth to highest

PreTreat

PreTreat

PreTreat

Average Sustained Pitting Rates

Average Penetration Depths

	Net Metal Recession (mil/year)							Cummulative Metal Recession (mil)						
	1 year	3 years	6 years	9 years	15 years	30 years	60 years	1 year	3 years	6 years	9 years	15 years	30 years	60 years
Titanium 6Al-4V	0.005	0.019	0.060	0.052	0.019	0.006	0.002	0.005	0.043	0.224	0.391	0.505	0.592	0.661
Titanium 6-4 LI	0.005	0.019	0.062	0.058	0.022	0.007	0.003	0.005	0.044	0.231	0.417	0.547	0.646	0.724
Titanium CP	0.004	0.013	0.043	0.069	0.035	0.009	0.003	0.004	0.031	0.159	0.366	0.582	0.724	0.828
Inconel 625	0.189	1.047	0.420	0.191	0.084	0.034	0.015	0.189	2.284	3.709	4.282	4.785	5.289	5.741
Hastelloy C-276	0.147	0.837	0.520	0.232	0.098	0.038	0.017	0.147	1.821	3.709	4.405	4.995	5.567	6.074
Cronidur 30	20.36	29.47	12.80	7.595	4.091	1.876	0.897	20.36	85.52	123.9	146.7	171.3	199.4	226.3

Pertains to actual etching into the base metal beyond repassivation recovery

Pertains to actual etching into the base metal beyond repassivation recovery

Ranked from lowest Pitting Depth to highest

Brine

Brine

Brine

Average Sustained Pitting Rates

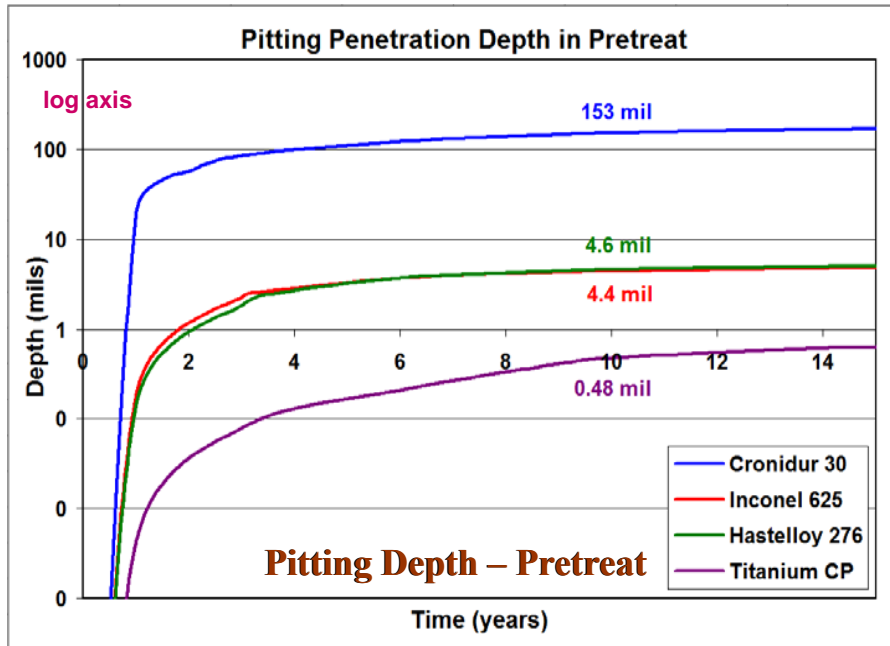
Average Penetration Depths

	Net Metal Recession (mil/year)							Cummulative Metal Recession (mil)						
	1 year	3 years	6 years	9 years	15 years	30 years	60 years	1 year	3 years	6 years	9 years	15 years	30 years	60 years
Titanium 6Al-4V	0.027	0.130	0.233	0.113	0.043	0.015	0.006	0.027	0.286	1.034	1.374	1.632	1.858	2.049
Titanium 6-4 LI	0.029	0.137	0.267	0.134	0.050	0.017	0.007	0.029	0.302	1.145	1.547	1.848	2.110	2.330
Titanium CP	0.021	0.077	0.239	0.189	0.068	0.021	0.008	0.021	0.175	0.892	1.506	1.915	2.233	2.485
Inconel 625	1.169	3.805	0.940	0.467	0.224	0.095	0.044	1.169	9.881	12.70	14.10	15.45	16.88	18.20
Hastelloy C-276	0.969	4.189	1.232	0.595	0.277	0.116	0.053	0.969	9.571	13.27	15.05	16.72	18.45	20.04
Cronidur 30	133.6	95.99	40.47	24.78	13.80	6.507	3.157	133.6	355.9	477.3	551.6	634.4	732.0	826.7

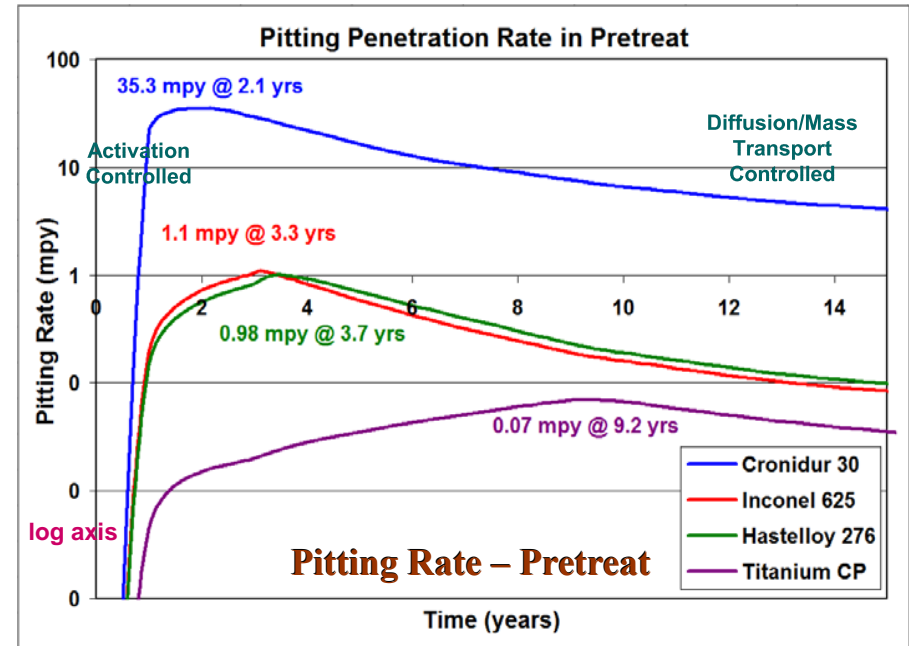
Pertains to actual etching into the base metal beyond repassivation recovery

Pertains to actual etching into the base metal beyond repassivation recovery

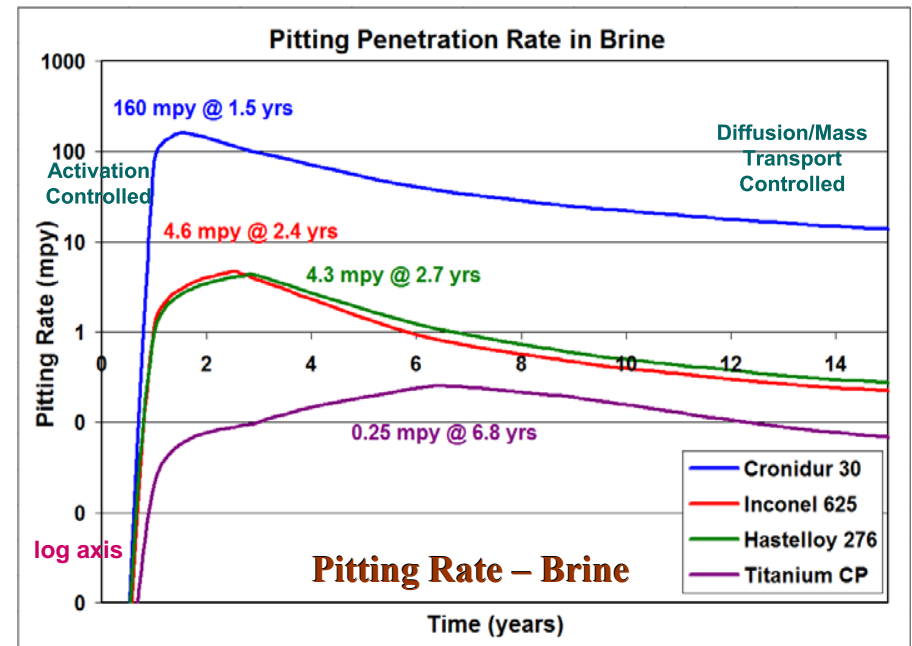
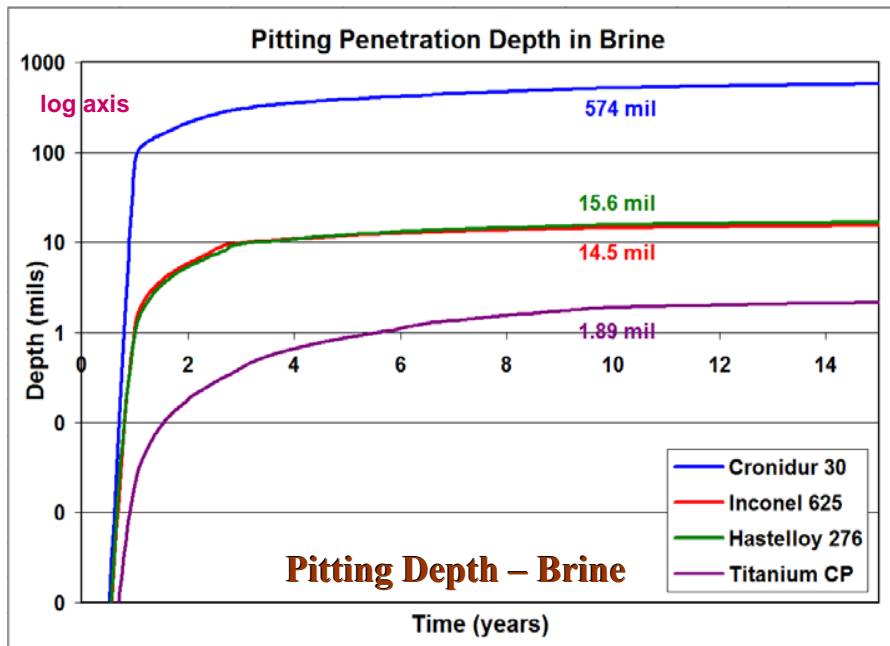
Model Pitting Rates and Pitting Depths for Worst Case Scenario



Pitting Depths asymptotically level off as repassivation increasingly dominates and the pitting rate eventually goes to zero



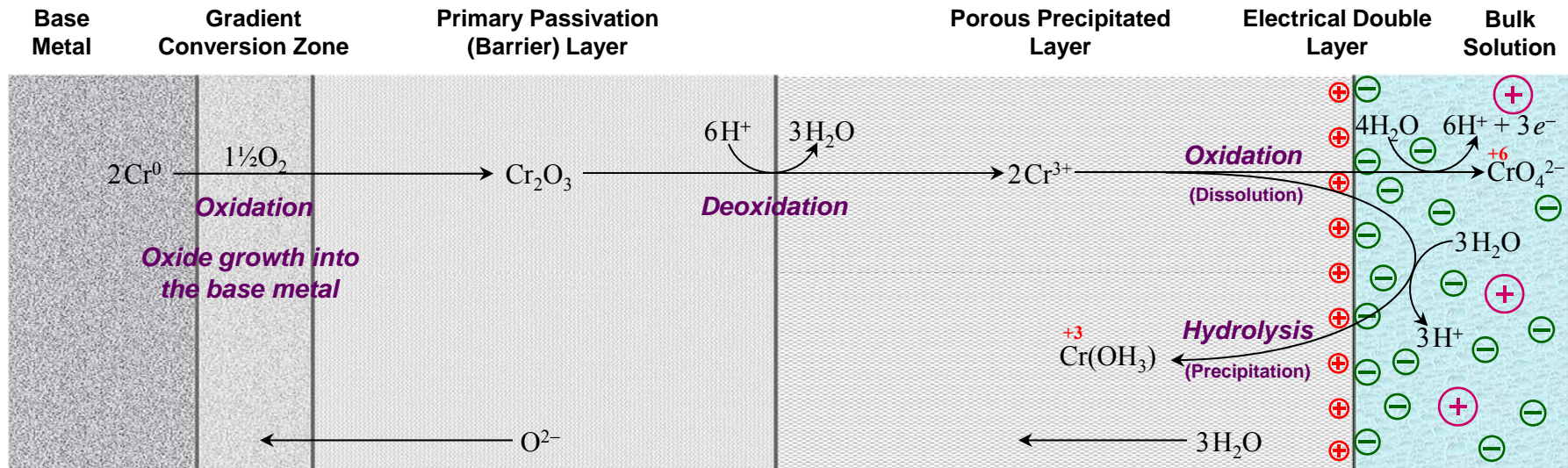
Pitting Rates are activation-controlled up to the maximum rate after which, rates become diffusion-controlled until they asymptotically cease



Description of Events Around the Breakdown Region (1 of 4)

At Steady State, The Oxide Forms and Dissolves at the Same Rate

- Our perception of the passivation phase on metals in aggressive solutions includes multiple layers with varying chemical processes and compositions. This can be simplified to a bilayer configuration for many evaluations where the (a) primary barrier / metal interface and the (b) precipitated layer / solution interface are recognized as the major regions of importance.



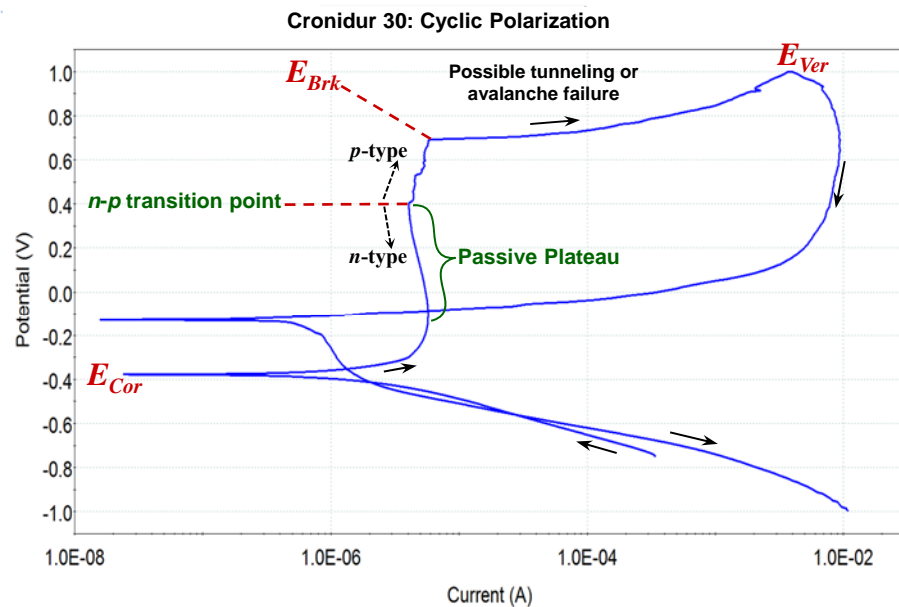
- The conversion zone is the region of transition between base metal and metal oxide. The primary barrier is the protective amorphous metal oxide phase. The precipitated phase is a porous, nonprotective gel-like structure that forms via hydrolysis of cations ejected from the barrier layer. The pore structure is columnar, providing for the passage of ions into and away from the barrier layer. The electrical double layer is the transition zone separating the porous layer from the solution and is formed to balance the positive charge on that surface. A loose layer of negative counterions accumulates at the surface and then a more diffuse region transitions into the bulk solution. Overall, the configuration is neutral in pH 7 solutions.

Description of Events Around the Breakdown Region (2 of 4)

Passive Films Treated as Pseudo $n-p$ Semiconductors

- There is a more comprehensive approach to understanding the kinetics and potential mechanisms associated with steady state growth and the breakdown of passive films. Elements from Macdonald's Point Defect Model* (PDM) should be introduced here.
- Mott-Schottky analysis has shown that the passive films on stainless steels, Ni-Cr alloys, Ti and its alloys exhibit the characteristics of a $p-n$ heterojunction with donor/acceptor densities on the order of $10^{20}/\text{cm}^3$. This value increases with decreasing pH, increasing temperature and increasing chloride concentration all of which lead to increased pitting susceptibility.
- The oxides are considered to contain an abundance of defects such as cation vacancies V_{Cr}^{3-} , oxygen vacancies $V_{\text{O}}^{\bullet\bullet}$ and cation interstitials $M_i^{\times\bullet}$ (as written in Kröger-Vink notation). The

oxide films behave as n -type semiconductors at potentials along the passive plateau where oxygen vacancies and cation interstitials are the dominant carriers.



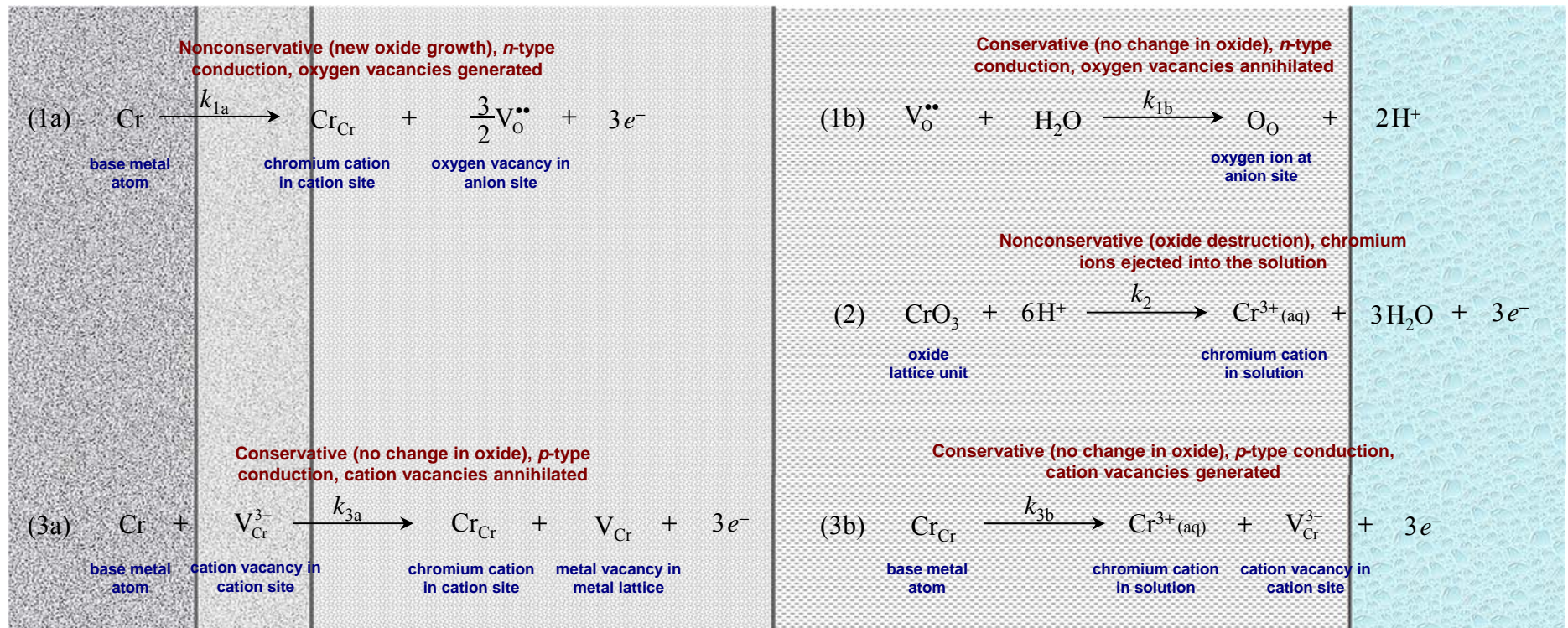
- Then there is a transition to p -type semiconductivity prior to E_{Brk} where cation lattice vacancies become the dominant carriers via ejection of cations into the solution. The current density increases slightly at the transition point just before complete breakdown occurs at E_{Brk} .

* The Point Defect Model, Digby D. Macdonald, Center for Advanced Materials, Penn. State University, University Park, PA, J. Electrochem. Soc., Vol. 139, No. 12, December 1992

Description of Events Around the Breakdown Region (3 of 4)

Passive Films Treated as Pseudo n - p Semiconductors

- The likely processes occurring during the passivation plateau and approaching E_{Brk} can be mapped out using Kröger-Vink notation with a chromium-rich oxide as before . . .



- Reactions (1a) and (2) represent the same reactions illustrated earlier where oxide is produced in the conversion zone and is hydrolyzed at the solution interface. At a passive steady state, these two nonconservative reactions balance each other out so that $k_{1a} = k_2$.
- Oxygen vacancies are created in (1a) and annihilated through reaction (1b). These carriers along with chromium interstitials (not shown) account for the n -type behavior exhibited during the passive state prior to the breakdown region.

Description of Events Around the Breakdown Region (4 of 4)

Passive Films Treated as Pseudo n - p Semiconductors

- At the n - p transition point, cation lattice carriers begin to dominate as the process switches to p -type behavior. These steps are depicted in reactions (3a) and (3b) where chromium vacancies are the primary carriers and chromium ions pass into solution.
- Reaction (3b) is expected to prevail while the level of cation vacancies increases, dissolution escalates and chromium ions are expelled into the solution. During and after the breakdown point, it is plausible that localized accumulation and agglomeration of cation vacancies within the conversion zone along the metal-barrier interface weaken the bonding links connecting base metal atoms to oxide units which leads to oxide separation and eventually pitting.
- The PDM provides several prediction tools regarding passivation and pitting and has shown that thickness changes in the oxide layer can be modelled using exponential forms. Our own work here has improvised similar descriptions for predicting rates based on measured current density I over time t , such as the generalized Weibull expressions alluded to earlier . . .

$$I = a - b \exp(-ct^{-d})$$

. . . where I is directly related to the rates of recession, passivation, dissolution and pitting, and where $a - b$ is equal to the projected limiting value at steady state.

- At present, much of this work is still ongoing. Refinement of the tools developed for this study as well as other concepts outlined in the PDM will be pursued in future studies with relevance to the types of metals and test environments of interest.